

DIVERSITY-ENHANCED AND CLASSIFICATION-AWARE PROMPT LEARNING FOR FEW-SHOT LEARNING VIA STABLE DIFFUSION

Anonymous authors

Paper under double-blind review

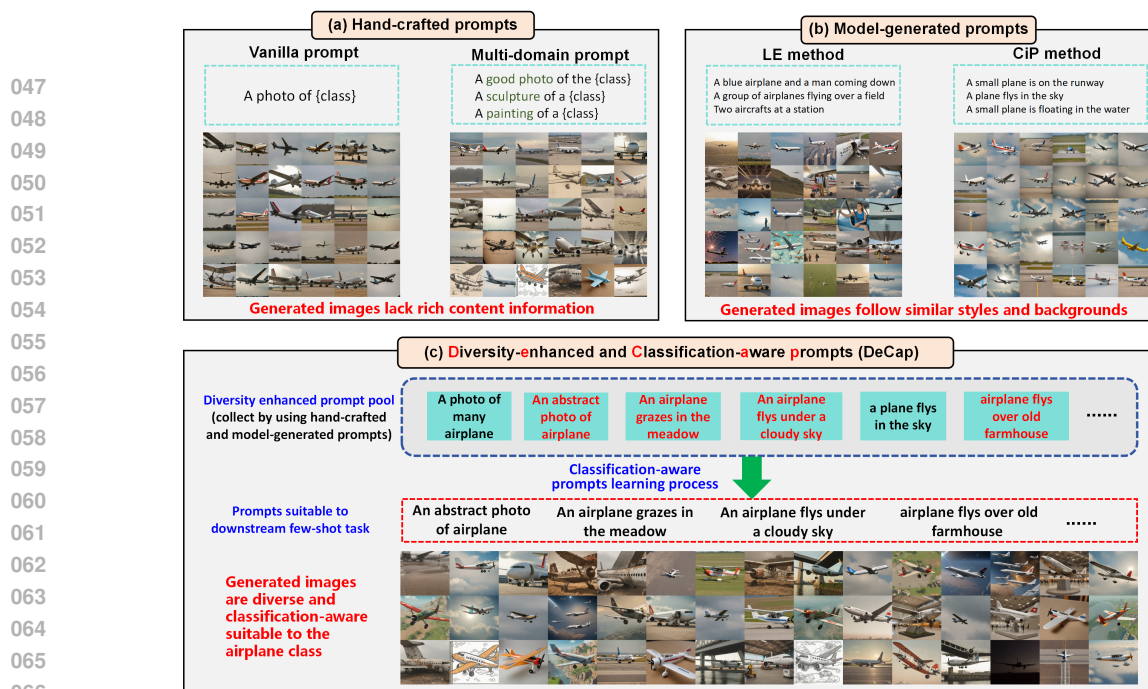
ABSTRACT

Recent text-to-image generative models have exhibited an impressive ability to generate fairly realistic images from some text prompts. In this work, we explore to leverage off-the-shelf text-to-image generative models to train non-specific downstream few-shot classification model architectures using synthetic dataset to classify real images. Current approaches use hand-crafted or model-generated text prompts of text-to-image generative models to generate desired synthetic images, however, they have limited capability of generating diverse images. Especially, their synthetic datasets have relatively limited relevance to the downstream classification tasks. This makes them fairly hard to guarantee training models from synthetic images are efficient in practice. To address this issue, we propose a method capable of adaptively learning proper text prompts for the off-the-shelf diffusion model to generate diverse and classification-aware synthetic images. Our approach shows notable improvements in various classification datasets, with results comparable to existing prompt designing methods. We find that replacing data generation strategy of existing zero/few-shot methods with proposed method could consistently improve downstream classification performance across different network architectures, demonstrating its model-agnostic characteristic for few-shot learning. This makes it possible to train an efficient downstream few-shot learning model from synthetic images generated by proposed method for real problems.

1 INTRODUCTION

Recently, deep learning powered by large-scale annotated data has achieved great success in the field of image recognition [17]. However, acquiring and curating a large-scale high-quality dataset can be notoriously costly and time-consuming. This is especially true for inherently expensive domains, such as medical imaging, remote sensing, etc. Few-shot learning addresses the data issue by training a model using few data from the concerned tasks [87; 72; 63]. Generally, few-shot learning models use specialised algorithms and architectures to achieve the objective [99; 60; 105; 3; 98; 67]. This limits the variety of model architectures and potential applicability for real-world problems.

An alternative approach is to generate a synthetic dataset which is then used to train a classification model. In the early period, some efforts [5; 103; 26] explored the use of GANs for data generation in image recognition. However, constrained by the limited generative capabilities of early GAN models, the synthetic datasets usually address tasks on a small scale or only for a specific setting. Recently, text-to-image foundation generative models, e.g., DALL-E [51], GLIDE [47], Imagen [56], and Stable Diffusion [54], which are trained on billions of image-text pairs from web-datasets, have demonstrated impressive breakthroughs in generating high-quality images from text descriptions. It is hopeful not only to generate high-quality labeled data, but also achieve domain customization to train a classifier model tailored for the concerned tasks.



067
068
069
070
071
072
073

Figure 1: The comparison between existing prompt designing methods and proposed DeCap method. Hand-crafted methods usually generate images with different domain information but limited content information. Model-generated methods overcome this shortcoming, while may generate images share similar patterns. DeCap constructs a diversity-enhanced prompt pool by integrating the advantages of hand-crafted and model-generated methods, and then carry out classification-aware prompt learning process to mine proper prompts suitable to downstream few-shot tasks. Figure shows the mined prompts for airplane classification.

074
075
076
077
078
079
080
081
082
083
084
085
086

To achieve the goal, some researchers pay attention to designing proper text descriptions (prompts) of text-to-image generation models to generate desired synthetic images. A direct approach is to construct prompts by formatting class labels according to a template (called vanilla prompt [57; 50]), such as “a photo of {class}”. To produce more diverse text descriptions, multi-domain prompt [62] additionally provides a list of domains with the prompt, e.g., “a {domain} of a {class}”, to construct a set of prompt templates, in which ‘{domain}’ refers to drawing, painting, sketch, etc. However, these hand-crafted prompts have limited capacity of generating images with rich content information, which usually leads to inferior generalization performance when training downstream models. To improve the content quality of prompts, the language enhancement (LE) method [18] leverages an off-the-shelf word-to-sentence T5 model to automatically expand class names into various sentences with rich content descriptions, containing the class names as language prompts. While this method hardly considers the class-relevant visual information for classification. The CiP method [37] generates high-quality prompts via extracting meaningful captions from real images using the off-the-shelf image captioning models such as BLIP2 [40], showing a significant improvement in generating informative synthetic images for better classification performance.

087
088
089
090
091
092
093

Although prompts produced by off-the-shelf foundational models can help generate high-quality images, they still have evident deficiencies in practice. On the one hand, generated prompts tend to share fixed or similar patterns for different images as reported in [82], which may limit diversity of synthetic images. For example, as shown in Figure 1, images generated by LE and CiP methods usually follow the similar styles and backgrounds. This limitation, which is even more serious under few-shot setting, may cause subpopulation shift problem [45; 92], i.e., some subpopulations of synthetic images shift from real-world datasets. On the other hand, existing prompt designing methods have relatively limited relevance to the

094 downstream classification tasks. Generally, the generated text prompts only employ class names or class-
095 relevant visual information, which leads to some noises in generated prompts, e.g., prompts containing noisy
096 labels or additional negative class information (please also see Figure 3). Therefore, it is relatively hard to
097 guarantee that training models from synthetic images are efficient for downstream classification tasks, which
098 tends to hinder their application effectiveness and reduce their performance stability in real problems.

099 To alleviate the aforementioned issues, this paper presents a **Diversity-enhanced** and **Classification-aware**
100 **prompt (DeCap)** learning strategy to mine proper text prompts for downstream few-shot classification tasks
101 (see Figure 1 for illustration). Our main idea is to combine existing hand-crafted diverse prompt tem-
102 plates and rich content prompt descriptions generated by off-the-shelf foundational models to construct a
103 prompt pool containing potentially all-inclusive diverse prompt information. And then we propose a novel
104 meta-learning approach to learn proper prompts tailored for the few-shot learning task. The DeCap method
105 involves two nested learning loops: an inner-loop to train a classification model using generated synthetic
106 images, and an outer-loop to search suitable prompts for text-to-image foundational generative models that
107 produce synthetic training data for the inner-level classification model. The few-shot images are employed to
108 compute outer-loop meta-objective for helping achieve classification-aware prompt learning. Through iter-
109 atively ameliorating both prompts selection and classification model performance, our algorithm is capable
110 of mining proper prompts which are attained specifically suitable to concerned few-shot learning task.

111 In summary, this paper makes the following three-fold contributions:

- 112 (1) We proposed to automatically learn proper text prompts for text-to-image generative models to generate
113 diverse and classification-aware synthetic images for few-shot learning task in a meta-learning manner.
- 114 (2) We verify that improving the diversity and classification-awareness of synthetic images could bring better
115 downstream few-shot classification performance compared with existing prompt designing methods.
- 116 (3) We show that replacing data generation strategy of existing zero/few-shot methods could further improve
117 downstream classification performance across different algorithms and network architectures.

118 The paper is organized as follows. Section 2 discusses related work. Section 3 presents the proposed method.
119 Section 4 demonstrates experimental results and the conclusion is finally made.

122 2 RELATED WORK

123 **Text-to-Image Diffusion Model.** Diffusion model [21; 71] has emerged as a research hotspot in the field
124 of image generation recently, due to their impressive generative capabilities. It achieves gradual matching
125 from a Gaussian distribution to an image distribution by reversing the diffusion process. Recently, thanks
126 to large-scale image-text paired datasets [59] and the maturity of text-image foundation models such as
127 CLIP, some state-of-the-art text-to-image diffusion models, including DALL-E [51], GLIDE [47], Imagen
128 [56], and Stable Diffusion [54], can produce a wide variety of highly realistic images, which has greatly
129 propelled research in fields such as art [81], style transfer [95; 102], image controlling [55; 100; 14], data
130 augmentation [77; 10] etc. In this paper, we explore leveraging off-the-shelf diffusion models to generate
131 high-quality synthetic images for downstream few-shot image recognition.

132 **Synthetic Dataset for Image Recognition.** In the early stages, some research[5; 103; 26] explored the role
133 of synthetic datasets with GAN models. However, due to the limited data generation capabilities of early
134 GANs, the application scenarios are significantly constrained. With the emergence of large-scale text-to-
135 image generative models, recent studies have validated the utility of synthetic datasets at a large scale. For
136 example, for classification tasks, [57; 4] train synthetic ImageNet datasets from scratch, [18; 38] showing
137 that CLIP [50] can boost performance from synthetic datasets. [76] validates the outstanding performance
138 of synthetic dataset using SimCLR and MAE models. In the field of object detection, [29] utilizes the output
139 results of generative model’s cross-attention layers as weak supervision for zero-shot object recognition.
140 Additionally, synthetic datasets are also applied to addressing long-tail problems [61].

The data generation strategy could be roughly divided into two categories. One is fine-tuning based method [2; 96], which fine-tunes generative models’ parameters using task data. These methods demonstrate strong domain adaptation capabilities on large-scale datasets and can effectively generate samples that conform to the distribution of real dataset. However, it often requires large-scale real datasets. Therefore, the other is prompt designing method to address few-shot learning. They don’t alter the parameters of generative models; instead, it focuses on setting proper prompts for off-the-shelf generative models to generate synthetic datasets. As discussed in Section 1, there exist two methodologies of setting prompts, i.e., hand-crafted and model-generated prompts. While they are not sufficient to generate high-quality images for classification. In this paper, we propose to integrate the advantages of both methodologies to achieve a diversity-enhanced and classification-aware prompt learning strategy. We need to clarify that, different from prompt learning methods [106; 107] specifically designed for multimodal models like CLIP, which directly helps adjust off-the-shell models prediction adapting to the concerned data, our prompt learning strategy focuses on generating efficient synthetic data for further help train downstream few-shot learning.

Meta Learning. Meta learning[22; 65], also known as learning to learn, focuses on how to quickly adapt and apply previously acquired knowledge when faced with new learning tasks. Meta learning is widely used in few-shot learning [12; 63; 52; 69], hyperparameter optimization [13], transfer learning [27; 74], label noise learning [64; 66; 89], machine learning automation [90], etc. For image generation field, meta learning is used to achieve data distillation [46; 86; 85; 73], data augmentation [91], etc. Different from previous works updating parameters of generative model, we use meta learning technique to learn proper text prompts of generative models to generate high-quality synthetic images for concerned few-shot learning task.

3 THE PROPOSED DECAP METHOD

3.1 PRELIMINARY

For a N -classification task, We use $\hat{x}_{ij}^{(k)} = g(\theta_{ij}, \epsilon_k)$ to denote the generated image $\hat{x}_{ij}^{(k)}$ via an off-the-shelf text-to-image foundational models g , where $i \in [N]$, $[N] = \{1, \dots, N\}$ represents the i -th class, $j \in [M]$, $[M] = \{1, \dots, M\}$, where M means how many different prompts for this class, θ_{ij} represents the prompt used to generate this image, ϵ_k represents random gaussian noise. We denote the mini dataset generated by prompt θ_{ij} as $X_{ij}^{syn} = \{\hat{x}_{ij}^{(k)}, k = 1, 2, \dots, l\}$, where l means the generation number of each prompt. We only study prompt setting for image generation, and we will drop explicit dependence of X_{ij}^{syn} on ϵ_k for brevity in the following, i.e., $X_{ij}^{syn} = g(\theta_{ij})$. Our approach can be directly applied to different diffusion models, and in this work we study the open-sourced model: Stable Diffusion (SD) [54].

Considering a few-shot classification task with real data $D^{real} = \{(x_{ij}, y_{ij}), i = 1, \dots, N, j = 1, \dots, K\}$, where x_{ij}, y_{ij} denote image and its label, and N, K denote the number of classes and samples of each class, respectively. To boost few-shot model performance, it could use SD model to help generate high-quality synthetic data for few-shot image recognition tasks. Specifically, the synthetic data could be formulated as

$$X^{syn} = g(\boldsymbol{\theta}), \boldsymbol{\theta} = \{\boldsymbol{\theta}_i, i \in [N]\}, \boldsymbol{\theta}_i = \{\theta_{i1}, \theta_{i2}, \dots, \theta_{iM}\}, X^{syn} = \{X_{ij}^{syn} = g(\theta_{ij}), i \in [N], j \in [M]\}.$$

For simplicity, we denote the obtained synthetic data as $D^{syn}(\boldsymbol{\theta}) = \{X^{syn}(\boldsymbol{\theta}), Y\}$, where $Y = \{Y_i, i \in [N]\}$, $Y_i = \{y_{i1}, \dots, y_{iM}\}$. Based on $D^{syn}(\boldsymbol{\theta})$, we could train a classification network f_w by optimizing the following objective:

$$w^* = \arg \min_{w \in \mathcal{W}} \mathcal{L}^{task}(f_w, D^{syn}(\boldsymbol{\theta})), \quad (1)$$

where \mathcal{W} denotes parameter space, $\mathcal{L}^{task}(f_w, D^{syn}(\boldsymbol{\theta})) = \frac{1}{MN} \sum_{i=1}^N \sum_{j=1}^M \mathcal{L}^{task}(f_w(x_{ij}), y_{ij})$, and \mathcal{L}^{task} denote the classification loss for the downstream few-shot learning task, e.g., cross-entropy loss.

As discussed in Section 1, existing prompt designing methods may generate limited diversity of synthetic images, tending to degrade generalization performance when training downstream classification models.

Especially, we could see that the prompt construction process of existing methods has limited relevance to the downstream classification tasks from Eq.(1), i.e., drops the explicit dependence of w^* on θ . In other words, existing prompt learning methods are classification-agnostic, which greatly reduces the alignment between synthetic datasets and downstream classification task requirement. To address these two issues, we propose a novel prompt learning strategy called DeCap, which explores to learn proper prompts for generating high-quality images to improve downstream few-shot learning task. We present the method and solving algorithm in Section 3.2 and 3.3, respectively.

3.2 PROPOSED DECAP METHOD

The proposed DeCap method firstly constructs a diversity-enhanced prompt pool (Section 3.2.1) by integrating the advantages of hand-crafted and model-generated methods, and then carry out classification-aware prompt learning process (Section 3.2.2) to mine proper prompts suitable to downstream few-shot task.

3.2.1 DIVERSITY-ENHANCED PROMPT POOL CONSTRUCTION

In this section, we proposed to integrate the advantages of both hand-crafted and model-generated methods to construct a prompt pool that contains potentially all-inclusive diverse prompt information.

Specifically, we construct a unique prompt pool Θ , which contains hand-crafted prompts and model generated prompts, for every class in the dataset. For hand-crafted prompts, we first select some common prompt templates provided by [50] which contain various domain information. Then we manually add some new prompts into the pool, covering aspects such as color, style, camera angle and so on. Since these prompts describe the object in general terms, we share these prompts for all classes. For model generated prompts, we use BLIP2 model as CiP method [37] to describe images from few-shot datasets, and utilize T5 model as LE method [18] to generate corresponding class prompts with class labels as information. These prompts describe the object in detail, so different classes will have totally different descriptions. In conclusion, for each category’s prompt θ_i , it consists of two parts: the hand-crafted prompt θ_i^h and the model-generated prompt θ_i^m , i.e., $\theta_i = [\theta_i^h, \theta_i^m]$, where all classes share the same template θ_i^h , while possess private prompt θ_i^m .

After conducting this process, there already exists adequate prompts containing both diverse domain and content information in the prompt pool. However, this prompt pool is overly abundant and classification-agnostic, which contains not only proper prompts but also noisy prompts for downstream few-shot learning task. An illustration of the necessity of using adaptive prompt learning please see Appendix D.1. Therefore, we further propose a classification-aware prompt learning strategy to mine proper prompts from the prompt pool in a meta-learning manner to help generate high-quality images suitable for downstream few-shot task. We give a simple example about what our prompt pool looks like in Appendix B.1.

3.2.2 CLASSIFICATION-AWARE PROMPT LEARNING

The main idea is to establish the direct connection between prompt setting process and downstream classification model learning. Inspired by recent meta learning methods [65; 73; 22], we formulate the classification-aware prompt learning as the following bi-level optimization objective:

$$\theta^* = \arg \min_{\theta \in \Theta} \mathcal{L}^{meta}(f_{w^*}(\theta), D^{real}), \quad (2)$$

$$\text{where } w^*(\theta) = \arg \min_{w \in \mathcal{W}} \mathcal{L}^{task}(f_w, D^{syn}(\theta)), \quad (3)$$

where the inner-level objective (Eq.(3)) is the same as Eq.(1), while we explicitly require the performance of classification model to depend on the prompts θ . Specifically, given a prompt set $\theta \in \Theta$, we use these prompts to obtain the synthetic dataset $D^{syn}(\theta)$, and then train the downstream classification model on the synthetic dataset. Different from existing method preassigning the prompts, we want to learn proper prompts to generate high-quality data that more suitable to downstream task. To this goal, we use few-shot data D^{real} given by the downstream tasks to compute the outer-level meta loss \mathcal{L}^{meta} for evaluating the performance

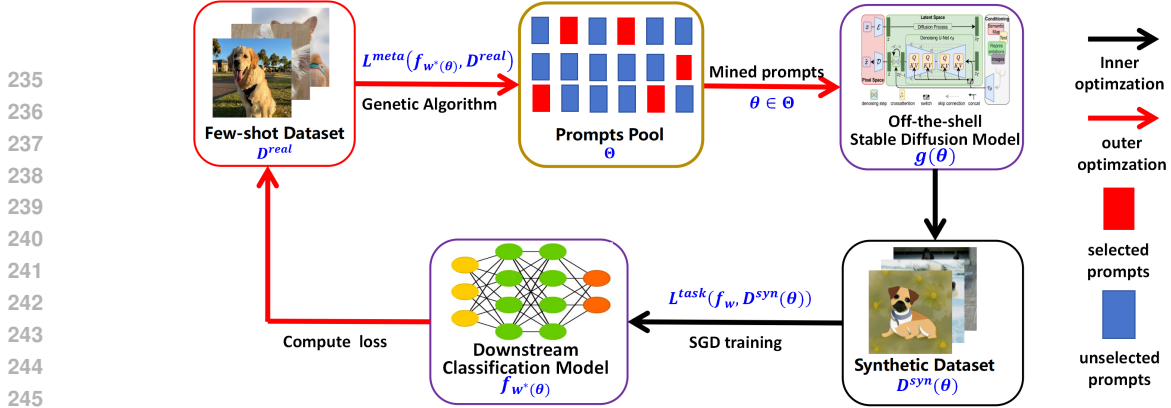


Figure 2: **Overview of the proposed DeCap method.** DeCap training involves two nested training loops. In the inner-loop optimization, we use the selected prompts set θ to generate synthetic dataset and then help train a downstream classification model, while in the outer-loop optimization, we search proper prompts from pre-constructed prompt pool which are attained specifically suitable to few-shot learning task.

Algorithm 1 Learning Algorithm of the Proposed DeCap Method

Input: Downstream few-shot learning task dataset D^{real} ; Algorithm iteration number $max-iter$, population quantity $popsize$; Prompt pool $pool$; off-the-shell text-to-image generative model g

Output: Optimal prompt set θ^*

```

1: GA.initial(max-iter,popsize)                                ▷ Genetic Algorithm (GA) initialize
2: for  $iter = 1, 2, \dots, max-iter$  do
3:   fitness=[], Pop=[]
4:   for  $m = 1, 2, \dots, popsize$  do
5:      $pop^{(m)} = GA.sample()$                                 ▷ An individual in the population
6:      $\theta^{(m)}, Y^{syn} = get\_prompt(pop^{(m)}, pool)$         ▷ See Algorithm 2 in Appendix B.2
7:      $X^{syn}(\theta^{(m)}) = g(\theta^{(m)})$ 
8:      $w^*(\theta^{(m)}) = \arg \min \mathcal{L}^{task}(f_w, D^{syn}(\theta^{(m)}))$   ▷ Inner-loop Optimization
9:      $fitness_{pop^{(m)}} = \mathcal{L}^{meta}(f_{w^*}(\theta^{(m)}), D^{real})$   ▷ Outer-loop Optimization
10:    fitness.append( $fitness_{pop^{(m)}}$ ), Pop.append( $pop^{(m)}$ )
11:  end for
12:  GA.update(fitness,Pop)                                     ▷ Updating searching direction
13: end for
14: return GA.best

```

of obtained classification model in Eq.(2), so as to learn proper prompts θ . Through iteratively ameliorating both searching prompts at outer-level learning and classification model performance at inner-level learning, our algorithm is capable of mining classification-aware prompts which is attained specifically suitable to downstream few-shot learning task. In our implementation, the optimization of $\theta \in \Theta$ is actually a discrete prompt selection problem. We will introduce the solving algorithm in the next section.

3.3 LEARNING ALGORITHM OF THE PROPOSED DECAP METHOD

Considering that the optimization of prompt θ is a discrete search problem, we use the genetic algorithm (GA) [31] to solve the outer-level optimization objective in Eq.(2). Generally speaking, a genetic algorithm first generates different inputs, then obtains the corresponding value function outputs for these inputs, adjusts the search direction based on the magnitude of the outputs, and eventually completes the optimization process. Therefore, we only need to define the GA's input and value function for DeCap objective, and then genetic algorithm can be employed to mine proper prompts θ^* from prompts pool Θ .

Table 1: Top-1 accuracy on different datasets. **Bold scores** represent the best result on each dataset, and the **second best scores** are marked by orange.

	STL-10	CIFAR10	Im-10	Pets	Caltech-101	Im-100	EuroSAT	Aircraft	Country211
<i>without real</i>									
zero-shot	94.26	70.25	97.22	81.85	83.89	70.14	23.11	17.07	13.44
vanilla prompt	95.33	72.37	97.69	82.29	84.74	70.62	31.31	17.04	13.72
multi-domain	94.97	70.66	97.89	83.07	87.56	70.50	30.11	17.85	13.90
LE	94.61	70.33	97.45	83.24	84.03	70.73	29.35	17.73	14.14
CiP	94.92	70.24	97.65	84.04	88.12	70.76	39.91	18.00	14.98
DeCap (ours)	95.91	76.98	97.95	85.36	88.67	71.08	41.94	19.74	15.44
<i>with real</i>									
real-only	94.28	70.33	97.22	81.96	84.51	70.33	24.15	19.41	13.80
vanilla prompt	95.55	76.20	98.00	83.84	89.85	70.87	47.83	18.21	13.77
multi-domain	95.02	74.54	97.92	84.56	90.31	70.62	43.30	18.99	13.90
LE	94.72	71.66	97.49	84.00	84.34	70.46	42.06	20.22	14.37
CiP	95.05	70.51	97.75	85.16	89.86	70.86	49.17	20.31	15.49
DeCap (ours)	95.93	77.19	98.03	85.78	89.87	71.11	50.22	20.64	15.68

In our problem, the input is defined as a vector of integers. The length of the vector represents the number of prompts selected, and each dimension of the vector corresponds to the index of the selected prompt, with values ranging from 0 to the size of the prompt pool. Under this definition, each input represents a different combination of selected prompts. The value function is defined as the outer-level meta loss \mathcal{L}^{meta} in Eq.(2).

For each category, the prompt θ_i includes the same hand-crafted prompts θ_i^h shared for all categories and the class-specific model-generated prompt θ_i^m . This hypothesis could effectively reduce the number of parameters for setting prompts. We believe this configuration is reasonable because domain information could typically be shared, while class-specific content descriptions cannot. Our DeCap method is able to balance the common patterns across categories with the unique differences specific to each category. The whole learning algorithm of proposed DeCap method is summarized in Algorithm 1. More details about genetic algorithm please see Appendix B.3.

4 EXPERIMENTAL RESULTS

4.1 FEW-SHOT CLASSIFICATION PERFORMANCE

We compared with existing prompt designing strategies including: (1) vanilla prompt [50]: using the template “a photo of {class}”. (2) multi-domain prompt: using different text templates from domains provided in [50]. (3) LE [18]: using the T5 model¹ for text prompt construction, where the input and output of T5 model are the class label and a sentence containing the class label, respectively. (4) CiP[37]: generating captions for real image data using the BLIP2² model. We conduct experiments on 9 datasets: CIFAR10[34], STL-10[7], Imagenette[24](Im-10), Pets[48], Caltech-101[11], ImageNet100[75](Im-100), EuroSAT[19], FGVC Aircraft[43] and Country211[50]. Datasets details are introduced in Appendix C.1. For the selection of the classification model, we use the CLIP model, as it has shown powerful classification ability. The training strategy we used strictly follows the settings described in [18], where we finetune CLIP with generated data. We use “a photo of {class}” as the text initialization for CLIP tuning for all datasets to eliminate the impact of different initializations on the evaluation of each method. Training and evaluating details are presented in Appendix C.2. Table 1 shows the few-shot classification performance of each method on six downstream few-shot learning datasets, where “without real” means that we only use synthetic datasets to train downstream models, while “with real” means that we use both synthetic and real few-shot images to train downstream models. Some ablation studies on DeCap method please see Appendix D.2.

Using synthetic data to train downstream classification model, DeCap method demonstrates the best classification accuracies across diverse datasets. All prompt designing methods can improve CLIP zero-shot per-

¹https://huggingface.co/mrm8488/t5-base-finetuned-common_gen

²<https://huggingface.co/Salesforce/blip2-opt-2.7b>

Table 2: Comparison of DeCap and SOTA methods on different datasets. “Method + DeCap” denotes the performance of replacing original synthetic data strategies of each method with DeCap method.

	STL-10	CIFAR10	Im-10	Pets	Caltech-101	Im-100	EuroSAT	Aircraft	Country211	average
FakeIt[57]	52.26	38.45	69.60	29.74	66.20	32.75	48.40	37.70	3.61	42.08
With DeCap	60.39	48.80	75.40	55.22	70.51	39.21	51.20	40.60	4.22	49.51
SuS-X[78]	95.24	72.77	98.24	79.64	84.57	69.96	33.89	18.30	12.96	62.84
With DeCap	95.43	75.89	98.39	80.40	84.89	70.3	37.37	19.83	13.02	63.94
CaFo[101]	95.33	85.34	97.66	86.62	94.09	74.64	83.5	26.07	16.20	73.28
With DeCap	95.90	86.00	98.06	88.66	94.28	76.28	84.46	26.76	16.88	74.14

formance, showing that generating synthetic data is helpful to train downstream classification model. As for datasets with simple categories like STL-10, CIFAR-10 and Im-10, the hand-crafted prompts could achieve superior performance than model-generated prompts, illustrating that the prompts with only class/domain information may be relatively more proper for these tasks; while for datasets with complex categories like Pets, Caltech-101 and Im-100, the model-generated prompts could achieve better performance than hand-crafted prompts, implying that rich content information is more helpful to address these complex tasks. These results reveal that effective prompts should be set based on concerned task information. To this goal, proposed DeCap method could adaptively learn proper prompts suitable to the concerned tasks by reconciling class/domain information and rich content information (visualization of mined prompts see Appendix E.2), so as to achieve an average performance improvement of 1.30% point compared to the best results of existing method on different datasets. We also evaluate the adversarial robustness of these methods in Appendix D.4, which further substantiate the high-quality data generation capability of DeCap method.

When using additional real data, CLIP’s performance could be further improved, though the number of real data is relatively smaller than synthetic data. This implies that the quality of real data may be higher than that of synthetic data. All prompt designing methods obtain a further improvement over only using synthetic data. Even so, DeCap method still shows advantages over other methods on most datasets, demonstrating that our approach could genuinely augment few-shot datasets. These experimental results support the capability of proposed DeCap method in generating high-quality images for downstream few-shot learning tasks.

4.2 COMPARISON WITH SOTA METHODS

In Section 4.1, we showed that under the same CLIP model architecture, DeCap performs well compared with other prompt designing methods. The key goal of DeCap method is to mine proper prompts to generate high-quality data for downstream few-shot learning, while it is not confined to specialised algorithms and architectures to complete few-shot learning tasks. To illustrate this, we explore to use synthetic data of DeCap method to evaluate its performance on other zero/few-shot algorithms and architectures.

Specifically, we conducted our experiments on three SOTA algorithms: (1) FakeIt [57]: It uses synthetic datasets to train the network on ResNet-50. (2) SuS-X [78]: It leverages synthetic datasets as a dynamic support set and extends Tip-Adapter by utilizing the image-text distance. (3) CaFo [101]: It augments few-shot datasets with synthetic data and then combines the predictions of pre-trained CLIP and DINO. In our implementations, we replaced the data generation strategies of these methods with DeCap without altering any of model architectures for a fair comparison, and follow original settings of these methods to train the corresponding classification models. More details please refer to Appendix C.3.

Table 2 reports the results. Notice that FakeIt method uses synthetic data to train the ResNet-50 model from scratch, which eliminates effects of pre-training data for downstream tasks. Thus performance of the trained classification model could appropriately reflect the quality of synthetic data. The DeCap method achieves a significant improvement of 7.43% point over original data generation strategy of FakeIt, substantiating the capability of our method in generating high-quality data suitable to concerned tasks. Though SuS-X and CaFo methods use pre-trained models, synthetic data of DeCap method could still outperform these methods in the vast majority of datasets. These results demonstrate that synthetic data of our DeCap method are not confined to specialised algorithms and architectures. This implies that our DeCap method is model-agnostic for downstream few-shot learning tasks, and hopeful to be readily applied to real-world problems and tasks.

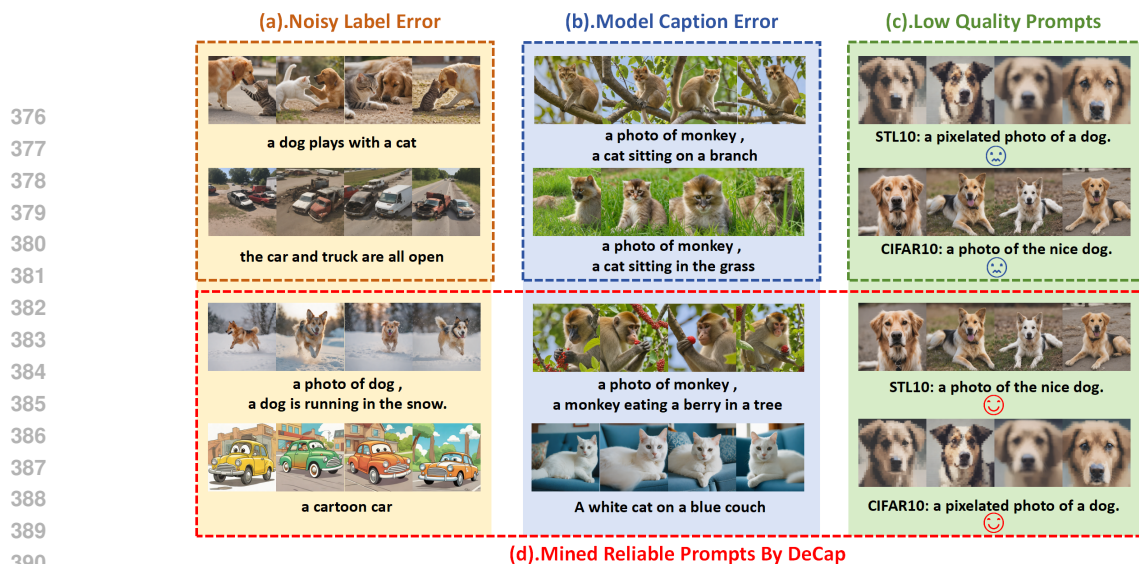


Figure 3: Illustration of (a) noisy label, (b) model caption error or (c) low quality prompts in prompt pool generated by existing prompt designing methods, and (d) mined reliable prompts by our DeCap method.

4.3 WHY PROPOSED DECAP METHOD PERFORM BETTER?

In this section, we further present some analysis of DeCap method in two aspects: robustness against noisy or low quality prompts, and data value analysis of synthetic data.

4.3.1 ROBUSTNESS AGAINST NOISY OR LOW QUALITY PROMPTS

Existing prompts methods may set noisy or low quality prompts for downstream tasks. For LE method, it may generate prompts that contain not only the class we want, but also other classes in the dataset. An illustrated example is presented in Fig.3 (a): for STL10 dataset, when we generate images for “dog”/“car” classes, some images also contain information of “cat”/“truck” classes. Since “cat”/“truck” classes belong to the dataset, these prompts would generate images with noisy labels for the classification of “dog”/“car”. For CiP method, due to the limitations of the BLIP2 model’s capability, it cannot always accurately annotate images, which may result in misidentifications. Although CiP method recognizes this issue and employs a prompt concatenation method like “a photo of {class}, {image caption}” to reduce the influence of noisy captions, we found this may not always work. For example, as shown in Fig.3 (b), when the BLIP2 model mistakenly identifies a monkey as a cat, the defined prompt “a photo of monkey, a cat sitting in a branch” may generate an image that blending features of cat and monkey. The issue of misidentification is particularly prominent in certain tasks, such as CIFAR10, where the low resolution images significantly impact the model’s judgments. This explains why the CiP method performs poorly on CIFAR10 dataset, as presented in Table 1. Moreover, hand-crafted prompts often introduce different domain information to construct diverse prompts. Generally, only part of domain information is reliable, while an amount of domain information may be of low quality for the concerned tasks. As shown in Fig.3 (c), though both of prompts could generate images of dog, the improper domain information could hinder the performance of concerned classification models, e.g., the synthetic pixelated images may provide low-quality training data for STL-10 task. In Appendix D.6, we further illustrate influence of prompts with domain information on the synthetic images.

Unfortunately, these noisy prompts are relatively hard to be filtered using data cleaning strategies such as CLIP filtering [18]. To address the issue, proposed DeCap method aims to mine proper prompts suitable to the concerned classification task in a meta-learning manner. As shown in Fig.3 (d), with such higher-level downstream classification-aware outer-loop supervised information, DeCap method could adaptively select effective prompts that help boost downstream classification performance, and discard aforementioned potential noisy prompts that would potentially hurt downstream classification performance.

423 424 425 426 427	a doodle of the car. 	dog walking on a sunny day. 	a photo of the bird. 	deer on a green pond. 
428 429 430 431 432 433 434 435 436	olympic athletes racing cars during racing match. 	a photo of dog , a dog is running in the snow 	a embroidered bird. 	a photo of the clean deer. 
437 438 439 440 441 442 443 444	A dynamic car. 	a photo of dog, a dog plays in water with stick 	art of the bird. 	a cartoon deer. 

Table 3: Examples of synthetic images generated by DeCap method for STL-10 dataset.

4.3.2 DATA VALUE ANALYSIS OF SYNTHETIC DATA

To better analyze why DeCap method outperforms existing prompt designing methods, we use “leave-one-out” method [16] to evaluate data valuation, and then select typical high-quality images generated by DeCap method. Specifically, given a dataset S and a measure function V , we use $\phi_i = V(D \cup \{i\}) - V(D)$ to represent data valuation of the synthetic image i . In our implementation, we use the dataset generated by vanilla prompt method as the benchmark dataset S and classification accuracy as the measure function V . Then we could compute data valuation of synthetic images generated by DeCap method via adding one image at a time. Table 3 visualizes the synthetic images with high data valuations for STL-10 dataset, and more visualizations are shown in Appendix E.1. As shown, we can see that synthetic images contain various patterns such as image style, background, camera angles, and actions, providing novel, diverse, and meaningful content information for original sparse data. This indicates that DeCap method does mine proper diverse and rich content prompts suitable to concerned downstream few-shot learning tasks, naturally leading to its better accuracy than other prompt designing methods.

5 CONCLUSION

We present the DeCap, a novel adaptive prompt learning approach to generate diverse and classification-aware synthetic data for downstream few-shot learning in a meta-learning manner. Proposed DeCap method could mine potential reliable prompts suitable to downstream few-shot learning tasks, demonstrating impressive capabilities in improving downstream classification models for different few-shot learning tasks compared with existing prompt designing methods. We could further boost existing SOTA zero/few-shot learning methods by simply replacing data generation strategy with the proposed method, showing its potential model-agnostic characteristics. Besides, we also provide some intuitive visual interpretation, providing an initial insight into proposed DeCap method. Such an adaptive prompt learning approach is hopeful to be employed to other computer vision tasks, like semantic segmentation and object detection, etc.

REFERENCES

- [1] Josh Achiam, Steven Adler, Sandhini Agarwal, Lama Ahmad, Ilge Akkaya, Florencia Leoni Aleman, Diogo Almeida, Janko Altenschmidt, Sam Altman, Shyamal Anadkat, et al. Gpt-4 technical report. *arXiv preprint arXiv:2303.08774*, 2023.
- [2] Shekoofeh Azizi, Simon Kornblith, Chitwan Saharia, Mohammad Norouzi, and David J Fleet. Synthetic data from diffusion models improves imagenet classification. *arXiv preprint arXiv:2304.08466*, 2023.
- [3] Sungyong Baik, Myungsub Choi, Janghoon Choi, Heewon Kim, and Kyoung Mu Lee. Learning to learn task-adaptive hyperparameters for few-shot learning. *IEEE Transactions on Pattern Analysis and Machine Intelligence*, 2023.
- [4] Hritik Bansal and Aditya Grover. Leaving reality to imagination: Robust classification via generated datasets. In *ICLR 2023 Workshop on Trustworthy and Reliable Large-Scale Machine Learning Models*, 2023. URL <https://openreview.net/forum?id=LjGqAFP6rA>.
- [5] Victor Besnier, Himalaya Jain, Andrei Bursuc, Matthieu Cord, and Patrick Pérez. This dataset does not exist: training models from generated images. In *ICASSP 2020-2020 IEEE International Conference on Acoustics, Speech and Signal Processing (ICASSP)*, pp. 1–5. IEEE, 2020.
- [6] Max F Burg, Florian Wenzel, Dominik Zietlow, Max Horn, Osama Makansi, Francesco Locatello, and Chris Russell. Image retrieval outperforms diffusion models on data augmentation. *Transactions on Machine Learning Research*, 2023.
- [7] Adam Coates, Andrew Ng, and Honglak Lee. An analysis of single-layer networks in unsupervised feature learning. In *Proceedings of the fourteenth international conference on artificial intelligence and statistics*, pp. 215–223. JMLR Workshop and Conference Proceedings, 2011.
- [8] Ekin D Cubuk, Barret Zoph, Dandelion Mane, Vijay Vasudevan, and Quoc V Le. Autoaugment: Learning augmentation strategies from data. In *Proceedings of the IEEE/CVF conference on computer vision and pattern recognition*, pp. 113–123, 2019.
- [9] Jia Deng, Wei Dong, Richard Socher, Li-Jia Li, Kai Li, and Li Fei-Fei. Imagenet: A large-scale hierarchical image database. In *2009 IEEE conference on computer vision and pattern recognition*, pp. 248–255. Ieee, 2009.
- [10] Lisa Dunlap, Alyssa Umno, Han Zhang, Jiezhi Yang, Joseph E Gonzalez, and Trevor Darrell. Diversify your vision datasets with automatic diffusion-based augmentation. *Advances in Neural Information Processing Systems*, 36, 2024.
- [11] Li Fei-Fei, Robert Fergus, and Pietro Perona. One-shot learning of object categories. *IEEE transactions on pattern analysis and machine intelligence*, 28(4):594–611, 2006.
- [12] Chelsea Finn, Pieter Abbeel, and Sergey Levine. Model-agnostic meta-learning for fast adaptation of deep networks. In *International conference on machine learning*, pp. 1126–1135. PMLR, 2017.
- [13] Luca Franceschi, Paolo Frasconi, Saverio Salzo, Riccardo Grazi, and Massimiliano Pontil. Bilevel programming for hyperparameter optimization and meta-learning. In *International conference on machine learning*, pp. 1568–1577. PMLR, 2018.
- [14] Rinon Gal, Yuval Alaluf, Yuval Atzmon, Or Patashnik, Amit H Bermano, Gal Chechik, and Daniel Cohen-Or. An image is worth one word: Personalizing text-to-image generation using textual inversion. *arXiv preprint arXiv:2208.01618*, 2022.

- 517 [15] Yaroslav Ganin, Evgeniya Ustinova, Hana Ajakan, Pascal Germain, Hugo Larochelle, François Lavi-
518 olette, Mario March, and Victor Lempitsky. Domain-adversarial training of neural networks. *Journal*
519 *of machine learning research*, 17(59):1–35, 2016.
- 520 [16] Amirata Ghorbani and James Zou. Data shapley: Equitable valuation of data for machine learning.
521 In *International conference on machine learning*, pp. 2242–2251. PMLR, 2019.
- 522 [17] Kaiming He, Xiangyu Zhang, Shaoqing Ren, and Jian Sun. Deep residual learning for image recog-
523 nition. In *CVPR*, 2016.
- 524 [18] Ruifei He, Shuyang Sun, Xin Yu, Chuhui Xue, Wenqing Zhang, Philip Torr, Song Bai, and Xiao-
525 juan Qi. Is synthetic data from generative models ready for image recognition? *arXiv preprint*
526 *arXiv:2210.07574*, 2022.
- 527 [19] Patrick Helber, Benjamin Bischke, Andreas Dengel, and Damian Borth. Eurosat: A novel dataset and
528 deep learning benchmark for land use and land cover classification. *IEEE Journal of Selected Topics*
529 *in Applied Earth Observations and Remote Sensing*, 12(7):2217–2226, 2019.
- 530 [20] Dan Hendrycks and Thomas Dietterich. Benchmarking neural network robustness to common corrup-
531 tions and perturbations. *Proceedings of the International Conference on Learning Representations*,
532 2019.
- 533 [21] Jonathan Ho, Ajay Jain, and Pieter Abbeel. Denoising diffusion probabilistic models. *Advances in*
534 *neural information processing systems*, 33:6840–6851, 2020.
- 535 [22] Timothy Hospedales, Antreas Antoniou, Paul Micaelli, and Amos Storkey. Meta-learning in neural
536 networks: A survey. *IEEE transactions on pattern analysis and machine intelligence*, 44(9):5149–
537 5169, 2021.
- 538 [23] Andrew G Howard, Menglong Zhu, Bo Chen, Dmitry Kalenichenko, Weijun Wang, Tobias Weyand,
539 Marco Andreetto, and Hartwig Adam. Mobilenets: Efficient convolutional neural networks for mobile
540 vision applications. *arXiv preprint arXiv:1704.04861*, 2017.
- 541 [24] Jeremy Howard and Sylvain Gugger. Fastai: a layered api for deep learning. *Information*, 11(2):108,
542 2020.
- 543 [25] Khawar Islam, Muhammad Zaigham Zaheer, Arif Mahmood, and Karthik Nandakumar. Diffusemix:
544 Label-preserving data augmentation with diffusion models. In *Proceedings of the IEEE/CVF Confer-*
545 *ence on Computer Vision and Pattern Recognition*, pp. 27621–27630, 2024.
- 546 [26] Ali Jahanian, Xavier Puig, Yonglong Tian, and Phillip Isola. Generative models as a data source for
547 multiview representation learning. *arXiv preprint arXiv:2106.05258*, 2021.
- 548 [27] Yunhun Jang, Hankook Lee, Sung Ju Hwang, and Jinwoo Shin. Learning what and where to transfer.
549 In *International conference on machine learning*, pp. 3030–3039. PMLR, 2019.
- 550 [28] Menglin Jia, Luming Tang, Bor-Chun Chen, Claire Cardie, Serge Belongie, Bharath Hariharan, and
551 Ser-Nam Lim. Visual prompt tuning. In *European Conference on Computer Vision*, pp. 709–727.
552 Springer, 2022.
- 553 [29] Laurynas Karazija, Iro Laina, Andrea Vedaldi, and Christian Rupprecht. Diffusion models for zero-
554 shot open-vocabulary segmentation. *arXiv preprint arXiv:2306.09316*, 2023.
- 555 [30] Laurynas Karazija, Iro Laina, Andrea Vedaldi, and Christian Rupprecht. Diffusion Models for Zero-
556 Shot Open-Vocabulary Segmentation. *arXiv preprint*, 2023.
- 557
558
559
560
561
562
563

- 564 [31] Sourabh Katoch, Sumit Singh Chauhan, and Vijay Kumar. A review on genetic algorithm: past,
565 present, and future. *Multimedia tools and applications*, 80:8091–8126, 2021.
- 566 [32] Hoki Kim. Torchattacks: A pytorch repository for adversarial attacks. *arXiv preprint*
567 *arXiv:2010.01950*, 2020.
- 569 [33] Diederik P Kingma and Max Welling. Auto-encoding variational bayes. *arXiv preprint*
570 *arXiv:1312.6114*, 2013.
- 571 [34] Alex Krizhevsky. Learning multiple layers of features from tiny images. Technical report, 2009.
- 572 [35] Alexey Kurakin, Ian J Goodfellow, and Samy Bengio. Adversarial examples in the physical world. In
573 *Artificial intelligence safety and security*, pp. 99–112. Chapman and Hall/CRC, 2018.
- 574 [36] Brenden M. Lake, Ruslan Salakhutdinov, and Joshua B. Tenenbaum. Human-level concept learning
575 through probabilistic program induction. *Science*, 350(6266):1332–1338, 2015. doi: 10.1126/science.
576 aab3050. URL <https://www.science.org/doi/abs/10.1126/science.aab3050>.
- 577 [37] Shiye Lei, Hao Chen, Sen Zhang, Bo Zhao, and Dacheng Tao. Image captions are natural prompts
578 for text-to-image models. *arXiv preprint arXiv:2307.08526*, 2023.
- 581 [38] Bo Li, Haotian Liu, Liangyu Chen, Yong Jae Lee, Chunyuan Li, and Ziwei Liu. Benchmarking and
582 analyzing generative data for visual recognition. *arXiv preprint arXiv:2307.13697*, 2023.
- 583 [39] Da Li, Yongxin Yang, Yi-Zhe Song, and Timothy M Hospedales. Deeper, broader and artier domain
584 generalization. In *Proceedings of the IEEE international conference on computer vision*, pp. 5542–
585 5550, 2017.
- 587 [40] Junnan Li, Dongxu Li, Caiming Xiong, and Steven Hoi. Blip: Bootstrapping language-image pre-
588 training for unified vision-language understanding and generation. In *International conference on*
589 *machine learning*, pp. 12888–12900. PMLR, 2022.
- 590 [41] Weixin Liang, Girmaw Abebe Tadesse, Daniel Ho, Li Fei-Fei, Matei Zaharia, Ce Zhang, and James
591 Zou. Advances, challenges and opportunities in creating data for trustworthy ai. *Nature Machine*
592 *Intelligence*, 4(8):669–677, 2022.
- 593 [42] Aleksander Madry, Aleksandar Makelov, Ludwig Schmidt, Dimitris Tsipras, and Adrian Vladu. To-
594 wards deep learning models resistant to adversarial attacks. In *International Conference on Learning*
595 *Representations*, 2018.
- 597 [43] S. Maji, J. Kannala, E. Rahtu, M. Blaschko, and A. Vedaldi. Fine-grained visual classification of
598 aircraft. Technical report, 2013.
- 599 [44] Chenlin Meng, Yutong He, Yang Song, Jiaming Song, Jiajun Wu, Jun-Yan Zhu, and Stefano Ermon.
600 Sdedit: Guided image synthesis and editing with stochastic differential equations. *arXiv preprint*
601 *arXiv:2108.01073*, 2021.
- 602 [45] Vaishnavh Nagarajan, Anders Andreassen, and Behnam Neyshabur. Understanding the failure modes
603 of out-of-distribution generalization. *arXiv preprint arXiv:2010.15775*, 2020.
- 604 [46] Timothy Nguyen, Zhoung Chen, and Jaehoon Lee. Dataset meta-learning from kernel ridge-
605 regression. *arXiv preprint arXiv:2011.00050*, 2020.
- 606 [47] Alexander Quinn Nichol, Prafulla Dhariwal, Aditya Ramesh, Pranav Shyam, Pamela Mishkin, Bob
607 Mcgrew, Ilya Sutskever, and Mark Chen. Glide: Towards photorealistic image generation and editing
608 with text-guided diffusion models. In *ICML*, 2022.
- 609
610

- 611 [48] Omkar M Parkhi, Andrea Vedaldi, Andrew Zisserman, and CV Jawahar. Cats and dogs. In *2012*
612 *IEEE conference on computer vision and pattern recognition*, pp. 3498–3505. IEEE, 2012.
- 613
- 614 [49] Ed Pizzi, Sreya Dutta Roy, Sugosh Nagavara Ravindra, Priya Goyal, and Matthijs Douze. A self-
615 supervised descriptor for image copy detection. In *Proceedings of the IEEE/CVF Conference on*
616 *Computer Vision and Pattern Recognition*, pp. 14532–14542, 2022.
- 617
- 618 [50] Alec Radford, Jong Wook Kim, Chris Hallacy, Aditya Ramesh, Gabriel Goh, Sandhini Agarwal,
619 Girish Sastry, Amanda Askell, Pamela Mishkin, Jack Clark, et al. Learning transferable visual models
620 from natural language supervision. In *International conference on machine learning*, pp. 8748–8763.
621 PMLR, 2021.
- 622 [51] Aditya Ramesh, Prafulla Dhariwal, Alex Nichol, Casey Chu, and Mark Chen. Hierarchical text-
623 conditional image generation with clip latents. 2022.
- 624
- 625 [52] Sachin Ravi and Hugo Larochelle. Optimization as a model for few-shot learning. In *International*
626 *conference on learning representations*, 2016.
- 627
- 628 [53] Benjamin Recht, Rebecca Roelofs, Ludwig Schmidt, and Vaishal Shankar. Do imagenet classifiers
629 generalize to imagenet? In *International conference on machine learning*, pp. 5389–5400. PMLR,
630 2019.
- 631
- 632 [54] Robin Rombach, Andreas Blattmann, Dominik Lorenz, Patrick Esser, and Björn Ommer. High-
633 resolution image synthesis with latent diffusion models. In *Proceedings of the IEEE/CVF conference*
634 *on computer vision and pattern recognition*, pp. 10684–10695, 2022.
- 635
- 636 [55] Nataniel Ruiz, Yuanzhen Li, Varun Jampani, Yael Pritch, Michael Rubinstein, and Kfir Aberman.
637 Dreambooth: Fine tuning text-to-image diffusion models for subject-driven generation. In *Proceed-*
638 *ings of the IEEE/CVF Conference on Computer Vision and Pattern Recognition*, pp. 22500–22510,
639 2023.
- 640
- 641 [56] Chitwan Saharia, William Chan, Saurabh Saxena, Lala Li, Jay Whang, Emily L Denton, Kamyar
642 Ghasemipour, Raphael Gontijo Lopes, Burcu Karagol Ayan, Tim Salimans, et al. Photorealistic
643 text-to-image diffusion models with deep language understanding. *Advances in neural information*
644 *processing systems*, 35:36479–36494, 2022.
- 645
- 646 [57] Mert Bulent Sariyildiz, Karteeek Alahari, Diane Larlus, and Yannis Kalantidis. Fake it till you make
647 it: Learning transferable representations from synthetic imagenet clones. In *Proceedings of the*
648 *IEEE/CVF Conference on Computer Vision and Pattern Recognition (CVPR)*, 2023.
- 649
- 650 [58] Axel Sauer, Dominik Lorenz, Andreas Blattmann, and Robin Rombach. Adversarial diffusion distil-
651 lation. *arXiv preprint arXiv:2311.17042*, 2023.
- 652
- 653 [59] Christoph Schuhmann, Romain Beaumont, Richard Vencu, Cade Gordon, Ross Wightman, Mehdi
654 Cherti, Theo Coombes, Aarush Katta, Clayton Mullis, Mitchell Wortsman, et al. Laion-5b: An open
655 large-scale dataset for training next generation image-text models. *Advances in Neural Information*
656 *Processing Systems*, 35:25278–25294, 2022.
- 657
- 658 [60] Marcin Sendera, Marcin Przewieźlikowski, Konrad Karanowski, Maciej Zieba, Jacek Tabor, and Prze-
659 myśław Spurek. Hypershot: Few-shot learning by kernel hypernetworks. In *WACV*, 2023.
- 660
- 661 [61] Joonghyuk Shin, Minguk Kang, and Jaesik Park. Fill-up: Balancing long-tailed data with generative
662 models. *arXiv preprint arXiv:2306.07200*, 2023.

- 658 [62] Jordan Shipard, Arnold Wiliem, Kien Nguyen Thanh, Wei Xiang, and Clinton Fookes. Diversity is
659 definitely needed: Improving model-agnostic zero-shot classification via stable diffusion. In *Proceed-*
660 *ings of the IEEE/CVF Conference on Computer Vision and Pattern Recognition (CVPR) Workshops*,
661 pp. 769–778, June 2023.
- 662 [63] Jun Shu, Zongben Xu, and Deyu Meng. Small sample learning in big data era. *arXiv preprint*
663 *arXiv:1808.04572*, 2018.
- 664 [64] Jun Shu, Qi Xie, Lixuan Yi, Qian Zhao, Sanping Zhou, Zongben Xu, and Deyu Meng. Meta-weight-
665 net: Learning an explicit mapping for sample weighting. *Advances in neural information processing*
666 *systems*, 32, 2019.
- 667 [65] Jun Shu, Deyu Meng, and Zongben Xu. Learning an explicit hyper-parameter prediction func-
668 tion conditioned on tasks. *J. Mach. Learn. Res.*, 24:186:1–186:74, 2021. URL <https://api.semanticscholar.org/CorpusID:258686161>.
- 669 [66] Jun Shu, Xiang Yuan, Deyu Meng, and Zongben Xu. Cmw-net: Learning a class-aware sample
670 weighting mapping for robust deep learning. *IEEE Transactions on Pattern Analysis and Machine*
671 *Intelligence*, 2023.
- 672 [67] Yang Shu, Zhangjie Cao, Jinghan Gao, Jianmin Wang, S Yu Philip, and Mingsheng Long. Omni-
673 training: bridging pre-training and meta-training for few-shot learning. *IEEE Transactions on Pattern*
674 *Analysis and Machine Intelligence*, 2023.
- 675 [68] Karen Simonyan and Andrew Zisserman. Very deep convolutional networks for large-scale image
676 recognition. *arXiv preprint arXiv:1409.1556*, 2014.
- 677 [69] Jake Snell, Kevin Swersky, and Richard Zemel. Prototypical networks for few-shot learning. *Ad-*
678 *vances in neural information processing systems*, 30, 2017.
- 679 [70] Kihyuk Sohn, Huiwen Chang, José Lezama, Luisa Polania, Han Zhang, Yuan Hao, Irfan Essa, and
680 Lu Jiang. Visual prompt tuning for generative transfer learning. In *Proceedings of the IEEE/CVF*
681 *Conference on Computer Vision and Pattern Recognition*, pp. 19840–19851, 2023.
- 682 [71] Yang Song and Stefano Ermon. Generative modeling by estimating gradients of the data distribution.
683 *Advances in neural information processing systems*, 32, 2019.
- 684 [72] Yisheng Song, Ting Wang, Puyu Cai, Subrota K Mondal, and Jyoti Prakash Sahoo. A comprehensive
685 survey of few-shot learning: Evolution, applications, challenges, and opportunities. *ACM Computing*
686 *Surveys*, 55(13s):1–40, 2023.
- 687 [73] Felipe Petroski Such, Aditya Rawal, Joel Lehman, Kenneth Stanley, and Jeffrey Clune. Generative
688 teaching networks: Accelerating neural architecture search by learning to generate synthetic training
689 data. In *International Conference on Machine Learning*, pp. 9206–9216. PMLR, 2020.
- 690 [74] Qianru Sun, Yaoyao Liu, Zhaozheng Chen, Tat-Seng Chua, and Bernt Schiele. Meta-transfer learning
691 through hard tasks. *IEEE Transactions on Pattern Analysis and Machine Intelligence*, 44(3):1443–
692 1456, 2020.
- 693 [75] Yonglong Tian, Dilip Krishnan, and Phillip Isola. Contrastive multiview coding. In *Computer Vision–*
694 *ECCV 2020: 16th European Conference, Glasgow, UK, August 23–28, 2020, Proceedings, Part XI*
695 *16*, pp. 776–794. Springer, 2020.

- 705 [76] Yonglong Tian, Lijie Fan, Phillip Isola, Huiwen Chang, and Dilip Krishnan. Stablerep: Synthetic
706 images from text-to-image models make strong visual representation learners. *Advances in Neural*
707 *Information Processing Systems*, 36, 2024.
- 708 [77] Brandon Trabucco, Kyle Doherty, Max Gurinas, and Ruslan Salakhutdinov. Effective data augmen-
709 tation with diffusion models. *arXiv preprint arXiv:2302.07944*, 2023.
- 710 [78] Vishaal Udandarao, Ankush Gupta, and Samuel Albanie. Sus-x: Training-free name-only transfer
711 of vision-language models. In *Proceedings of the IEEE/CVF International Conference on Computer*
712 *Vision*, pp. 2725–2736, 2023.
- 713 [79] Ashish Vaswani, Noam Shazeer, Niki Parmar, Jakob Uszkoreit, Llion Jones, Aidan N Gomez, Łukasz
714 Kaiser, and Illia Polosukhin. Attention is all you need. *Advances in neural information processing*
715 *systems*, 30, 2017.
- 716 [80] Catherine Wah, Steve Branson, Peter Welinder, Pietro Perona, and Serge Belongie. *The Caltech-*
717 *UCSD Birds-200-2011 Dataset*. 7 2011.
- 718 [81] Risqo Wahid, Joel Mero, and Paavo Ritala. Written by chatgpt, illustrated by midjourney: generative
719 ai for content marketing. *Asia Pacific Journal of Marketing and Logistics*, 35(8):1813–1822, 2023.
- 720 [82] Alex Jinpeng Wang, Kevin Qinghong Lin, David Junhao Zhang, Stan Weixian Lei, and Mike Zheng
721 Shou. Too large; data reduction for vision-language pre-training. In *Proceedings of the IEEE/CVF*
722 *International Conference on Computer Vision*, pp. 3147–3157, 2023.
- 723 [83] Boyu Wang, Jorge A Mendez, Changjian Shui, Fan Zhou, Di Wu, Gezheng Xu, Christian Gagné,
724 and Eric Eaton. Gap minimization for knowledge sharing and transfer. *Journal of Machine Learning*
725 *Research*, 24(33):1–57, 2023.
- 726 [84] Haohan Wang, Songwei Ge, Zachary Lipton, and Eric P Xing. Learning robust global representations
727 by penalizing local predictive power. In *Advances in Neural Information Processing Systems*, pp.
728 10506–10518, 2019.
- 729 [85] Kai Wang, Jianyang Gu, Daquan Zhou, Zheng Zhu, Wei Jiang, and Yang You. Dim: Distilling dataset
730 into generative model. *arXiv preprint arXiv:2303.04707*, 2023.
- 731 [86] Tongzhou Wang, Jun-Yan Zhu, Antonio Torralba, and Alexei A Efros. Dataset distillation. *arXiv*
732 *preprint arXiv:1811.10959*, 2018.
- 733 [87] Yaqing Wang, Quanming Yao, James T Kwok, and Lionel M Ni. Generalizing from a few examples:
734 A survey on few-shot learning. *ACM computing surveys*, 53(3):1–34, 2020.
- 735 [88] Zhicai Wang, Longhui Wei, Tan Wang, Heyu Chen, Yanbin Hao, Xiang Wang, Xiangnan He, and
736 Qi Tian. Enhance image classification via inter-class image mixup with diffusion model. In *Proceed-*
737 *ings of the IEEE/CVF Conference on Computer Vision and Pattern Recognition*, pp. 17223–17233,
738 2024.
- 739 [89] Yichen Wu, Jun Shu, Qi Xie, Qian Zhao, and Deyu Meng. Learning to purify noisy labels via meta
740 soft label corrector. In *Proceedings of the AAAI Conference on Artificial Intelligence*, volume 35, pp.
741 10388–10396, 2021.
- 742 [90] Zongben Xu, Jun Shu, and Deyu Meng. Simulating learning methodology (slem): an approach to
743 machine learning automation. *National Science Review*, 11(8):nwae277, 2024.
- 744
745
746
747
748
749
750
751

- 752 [91] Shin'ya Yamaguchi, Daiki Chijiwa, Sekitoshi Kanai, Atsutoshi Kumagai, and Hisashi Kashima. Reg-
753 ularizing neural networks with meta-learning generative models. *Advances in Neural Information*
754 *Processing Systems*, 36, 2024.
- 755 [92] Yuzhe Yang, Haoran Zhang, Dina Katabi, and Marzyeh Ghassemi. Change is hard: A closer look at
756 subpopulation shift. In *ICML*, 2023.
- 757 [93] Zuhao Yang, Fangneng Zhan, Kunhao Liu, Muyu Xu, and Shijian Lu. Ai-generated images as data
758 source: The dawn of synthetic era. *arXiv preprint arXiv:2310.01830*, 2023.
- 759 [94] Zhuoran Yu, Chenchen Zhu, Sean Culatana, Raghuraman Krishnamoorthi, Fanyi Xiao, and Yong Jae
760 Lee. Diversify, don't fine-tune: Scaling up visual recognition training with synthetic images. *arXiv*
761 *preprint arXiv:2312.02253*, 2023.
- 762 [95] Jianhao Yuan, Francesco Pinto, Adam Davies, and Philip Torr. Not just pretty pictures: Toward
763 interventional data augmentation using text-to-image generators. *arXiv preprint arXiv:2212.11237*,
764 2022.
- 765 [96] Jianhao Yuan, Jie Zhang, Shuyang Sun, Philip Torr, and Bo Zhao. Real-fake: Effective training data
766 synthesis through distribution matching. *arXiv preprint arXiv:2310.10402*, 2023.
- 767 [97] Sergey Zagoruyko and Nikos Komodakis. Wide residual networks. *arXiv preprint arXiv:1605.07146*,
768 2016.
- 769 [98] Baoquan Zhang, Xutao Li, Yunming Ye, and Shanshan Feng. Prototype completion for few-shot
770 learning. *IEEE Transactions on Pattern Analysis and Machine Intelligence*, 2023.
- 771 [99] Ji Zhang, Lianli Gao, Xu Luo, Hengtao Shen, and Jingkuan Song. Deta: Denoised task adaptation for
772 few-shot learning. In *ICCV*, 2023.
- 773 [100] Lvmin Zhang, Anyi Rao, and Maneesh Agrawala. Adding conditional control to text-to-image dif-
774 fusion models. In *Proceedings of the IEEE/CVF International Conference on Computer Vision*, pp.
775 3836–3847, 2023.
- 776 [101] Renrui Zhang, Xiangfei Hu, Bohao Li, Siyuan Huang, Hanqiu Deng, Yu Qiao, Peng Gao, and Hong-
777 sheng Li. Prompt, generate, then cache: Cascade of foundation models makes strong few-shot learn-
778 ers. In *Proceedings of the IEEE/CVF Conference on Computer Vision and Pattern Recognition*, pp.
779 15211–15222, 2023.
- 780 [102] Yuxin Zhang, Nisha Huang, Fan Tang, Haibin Huang, Chongyang Ma, Weiming Dong, and Chang-
781 sheng Xu. Inversion-based style transfer with diffusion models. In *Proceedings of the IEEE/CVF*
782 *conference on computer vision and pattern recognition*, pp. 10146–10156, 2023.
- 783 [103] Yuxuan Zhang, Huan Ling, Jun Gao, Kangxue Yin, Jean-Francois Lafleche, Adela Barriuso, Antonio
784 Torralba, and Sanja Fidler. Datasetgan: Efficient labeled data factory with minimal human effort. In
785 *Proceedings of the IEEE/CVF Conference on Computer Vision and Pattern Recognition*, pp. 10145–
786 10155, 2021.
- 787 [104] Chenyu Zheng, Guoqiang Wu, and Chongxuan Li. Toward understanding generative data augmenta-
788 tion. *Advances in neural information processing systems*, 36:54046–54060, 2023.
- 789 [105] Fei Zhou, Peng Wang, Lei Zhang, Wei Wei, and Yanning Zhang. Revisiting prototypical network for
790 cross domain few-shot learning. In *CVPR*, 2023.
- 791
792
793
794
795
796
797
798

799 [106] Kaiyang Zhou, Jingkang Yang, Chen Change Loy, and Ziwei Liu. Conditional prompt learning for
800 vision-language models. In *Proceedings of the IEEE/CVF conference on computer vision and pattern*
801 *recognition*, pp. 16816–16825, 2022.

802 [107] Kaiyang Zhou, Jingkang Yang, Chen Change Loy, and Ziwei Liu. Learning to prompt for vision-
803 language models. *International Journal of Computer Vision*, 130(9):2337–2348, 2022.

804 [108] Yongchao Zhou, Hshmat Sahak, and Jimmy Ba. Training on thin air: Improve image classification
805 with generated data. *arXiv preprint arXiv:2305.15316*, 2023.

806

807

808

809

810

811

812

813

814

815

816

817

818

819

820

821

822

823

824

825

826

827

828

829

830

831

832

833

834

835

836

837

838

839

840

841

842

843

844

845

846 A LIMITATIONS

847
848
849 Although our DeCap method performs well among different datasets and model architectures compared
850 with existing prompt designing methods, we have to admit that DeCap has the following limitations. Firstly,
851 DeCap requires more training cost. It usually spends 160 GPU hours to mine proper prompts on small
852 scale datasets such as STL-10 and CIFAR10, and for large scale datasets such as Imagenet100, the cost
853 will go up to nearly 700 GPU hours. However, it is worth emphasizing that once we finish training, the
854 prompts we have learned could be used to generate sufficient images for training other few-shot algorithms
855 and model architectures. Secondly, the search space of prompt set for DeCap method is confined to the
856 pre-constructed prompt pool, which may lead to suboptimal solutions. One potential strategy is to learn
857 continuous soft prompts just like what [28; 107; 70] do. However, the computation of meta gradients for
858 learning soft prompts requires unaffordable memory: even a Nvidia A800 GPU can't support the backward
859 of a single synthetic image. Note that the suboptimal solutions of DeCap method could achieve impressive
860 performance, we believe more advanced prompt learning strategy would further boost the downstream clas-
861 sification models. Lastly, compared with model-generated prompt methods, proposed DeCap method seems
862 to lack extensibility. One promising idea is to learn a prompt generator that produces prompts conditioned
863 on concerned tasks. We leave the above potential shortcomings for future work, and we also look forward
864 to the emergence of following works to address these problems.

865 B MORE DETAILS OF PROPOSED DECAP METHOD

866 B.1 EXAMPLES OF PROMPT POOL CONSTRUCTION

867
868
869 In this section, we give a simple example about what our prompt pool looks like.

870 Let us consider “cat v.s. dog” classification task. Assuming that our hand-crafted prompts are [“a photo of
871 {}”, “a sketch of {}”, “a {} image”] and model-generated prompts are {cat:[“a cat on the grass”, “a cute cat
872 ”], dog:[“a barking dog”, “a dog in the room”]}. Then, our prompt pool will be:

873
874
875 {cat:[“a photo of {cat}”, “a sketch of {cat}”, “a {cat} image”, “a cat on the grass”, “a cute cat”],
876 dog:[“a photo of {dog}”, “a sketch of {dog}”, “a {dog} image”, “a barking dog”, “a dog in the room”]}

877
878 If we randomly select 2 prompts for each class, for example, the 0th and 3th prompts for cat, and 1th and
879 2th prompts for dog, which represents $pop = [0, 3, 1, 2]$, the selected prompts for generating dataset will be
880 {cat:[“a photo of {cat}”, “a cat on the grass”]; dog:[“a sketch of {dog}”, “a {dog} image”]}.

881 If we share hand-crafted prompts, for example, assuming we select the prompt template “a photo of {}”,
882 then it means that [“a photo of {cat}”, “a photo of {dog}”] will be selected to help generate dataset.

883 B.2 “GET_PROMPT” METHOD IN ALGORITHM 1

884
885
886
887
888
889
890
891 Algorithm 2 shows the “get_prompt” method in Algorithm 1. We denote the number of classes as N , the
892 name of these classes as “class_names”, prompt numbers per class as M .

Algorithm 2 Get_prompt Algorithm

Input: indexes pop , prompt pool $pool$; hyper-parameters including: whether share hand-crafted prompts $share$, hand-crafted prompts numbers n ;

Output: prompt set: prompts, labels: Y^{syn}

```

1: pop.reshape[ $N, M$ ]           ▷ pop is the index of  $\theta = [\theta_1, \theta_2, \dots, \theta_N]^T, \theta_i \in \mathbb{R}^M$  in prompt pool
2: if  $share$  then
3:   pop[:, :  $n$ ]=pop[0, :  $n$ ].repeat[ $N, 1$ ]           ▷ we make all the first  $n$  elements of  $\theta_i$  the same
4: end if
5: prompts=[],  $Y^{syn}$ =[]           ▷  $Y^{syn}$  contains every synthetic sample's label
6: for  $i = 1, 2, \dots, N$  do
7:   class=class_names[ $i$ ]
8:   prompts.append( $pool[class][pop[i]]$ )
9:    $Y^{syn}$ .append( $i$ .repeat[ $M$ ])
10: end for
11: return prompts,  $Y^{syn}$ 

```

B.3 GA ALGORITHM DETAILS

Genetic Algorithm (GA) is an optimization technique inspired by natural selection and genetic processes, widely used for complex problem-solving. Its key steps can be summarized as follows:

- Initialization of Population: Randomly generate a set number of individuals (solutions) to form the initial population, with each individual represented by a gene encoding (typically a binary string or real numbers).
- Fitness Evaluation: Assess the fitness of each individual using a fitness function that quantifies their performance based on the problem's objectives.
- Selection: Select individuals for the next generation based on their fitness values. Common selection methods include roulette wheel selection, tournament selection, and rank selection, where fitter individuals have a higher chance of being chosen.
- Crossover: Combine parts of two parent individuals' genes to produce new offspring. Crossover enhances genetic diversity, with methods like single-point, multi-point, and uniform crossover.
- Mutation: Introduce random changes to a portion of an individual's genes with a certain probability, increasing genetic variation and helping to avoid local optima. Mutation can involve flipping gene bits or assigning random values.
- Population Update: Merge the offspring with the current population and select suitable individuals based on fitness, often using elitism to retain the best solutions.
- Termination Condition: Determine if termination criteria are met, such as reaching a maximum number of iterations, achieving a predefined fitness goal, or when improvements in fitness become negligible.
- Output Results: Present the final optimal solution or any satisfactory solutions, along with relevant analysis and validation.

Actually, in Algorithm 1, the $GA.update()$ operation means the steps from "selection" to "population update" operation. Our code are based on the scikit-opt library, and we use their default operators. What's more, unlike traditional meta learning methods[12; 63; 13; 27; 74] relying on computing meta gradient to optimize outer-level meta loss, our outer-level optimization does not involve any meta gradient calculation (i.e., derivative-free optimization), and we only execute gradient descent algorithm at the inner-level optimization.

C IMPLEMENTATION DETAILS

C.1 DATASETS DETAILS

In this section, we give a brief introduction about datasets we used in Section 4.

CIFAR10: The CIFAR10 dataset contains 10 common classes: airplane, car, bird, cat, dog, deer, frog, horse, ship, truck. Each class contains 6000 color images with 32×32 size. CIFAR10 is widely used in image classification.

STL-10: The STL-10 dataset contains 10 common classes in real life: airplane, bird, car, cat, deer, dog, horse, monkey, ship, and truck. Although these photos comes from ImageNet, their annotations may be quite different, for example, “dog” class contains various dog breeds.

Imagenette: Imagenette is a subset of the larger ImageNet dataset, containing 10 easily distinguished classes: tench, English springer, cassette player, chain saw, church, French horn, garbage truck, gas pump, golf ball, parachute. It was created to provide a smaller, more manageable subset for training and testing image classification models.

Pets: The Pets dataset consists of images of 12 different cats breeds and 25 different dogs breeds. It is commonly used for fine-grained classification tasks, where the goal is to classify images into specific sub-categories within a broader class.

ImageNet100: ImageNet100 is a subset of the original ImageNet dataset, containing 100 classes. It serves as a smaller alternative to the full ImageNet dataset for training and evaluating deep learning models for image classification tasks.

Caltech-101: The Caltech-101 dataset is a widely used benchmark dataset for object recognition. It contains images of objects belonging to 101 distinct categories, including animals, vehicles, and household items.

EuroSAT: EuroSAT is a dataset of Sentinel-2 satellite images for land cover classification. It contains 27,000 RGB images across 10 classes, such as agriculture, forest, and water bodies, with a resolution of 64×64 pixels. It is widely used in remote sensing and environmental monitoring tasks.

Aircraft: The FGVC Aircraft dataset is designed for fine-grained visual classification of aircraft. It includes 10,000 images of 102 different aircraft models, focusing on distinguishing subtle differences between similar models. It is commonly used in fine-grained recognition research.

Country211: Country211 is a dataset released by OpenAI, designed to assess the geolocation capability of visual representations. It filters the YFCC100m dataset to find 211 countries that have at least 300 photos with GPS coordinates. OpenAI built a balanced dataset with 211 categories, by sampling 200 photos for training and 100 photos for testing, for each country.

C.2 EXPERIMENT SETTINGS IN SECTION 4.1

C.2.1 MODEL SELECTION

For the pre-trained generative model, we choose the Stable Diffusion XL-Turbo (SDXL-Turbo) model³ for its fast generation speed and high quality image generation. This model takes text prompts as input and outputs images at a resolution of 512×512 . During our experiments, we use ResNet-50 as the CLIP image encoder backbone. For classifier tuning [18], different text prompt initializations may cause slight differences in accuracy, but since our method focuses on the dataset quality, we simply use the vanilla template “a photo of {class}” for all the datasets.

³<https://huggingface.co/stabilityai/sdxl-turbo>

987 C.2.2 TRAINING SETTING

988 Since Stable Diffusion XL-Turbo doesn't use Classifier-free guidance, we simply set the guidance scale to
 989 0 and we set inference steps to 2. For inner training of classification model, we generated 80 images for
 990 each class and trained for 20 epochs using the Adam optimizer with a learning rate from $2e - 3$ to $2e - 5$,
 991 equipped with the Cosine learning rate schedule. For outer training, we set the hyper-parameters of the GA
 992 algorithm as follows: popsize of 80, maxiter of 80.
 993

994 Regarding the selection of few-shot datasets, we randomly selected 10 images per class to form the few-shot
 995 datasets. For CIFAR10, STL-10, Imagenette, EuroSAT we learn 20 prompts for each class, while for others,
 996 we use the technique mentioned in the Section 3.3 and learned 10 common prompts and 10 class-specific
 997 prompts for each class. We do training on 8 NVIDIA A800 GPUs, with pytorch 1.12.1 and Ubuntu 20.04.
 998

999 C.2.3 EVALUATION SETTINGS

1000 Stable Diffusion model settings are the same in Appendix C.2.2. We generated 800 images for each class
 1001 and fine-tune CLIP for 30 epochs. We use the the Adam optimizer equipped with the Cosine schedule. After
 1002 training, we use the fine-tuned CLIP model to do evaluation on real test datasets. All the results are the
 1003 average over 5 times run, with random seed in 7, 21, 42, 84, 105.
 1004

1005 C.3 EXPERIMENT SETTINGS IN SECTION 4.2

1006
 1007 **FakeIt:** FakeIt use Stable Diffusion V1-4 model and different classifier-free guidance scale, but our gen-
 1008 erative model are not fit for using classifier-free guidance, so we re-implemented their generation approach
 1009 under our generative model. Other training settings are the same with original paper, including classification
 1010 model architecture, training learning rate, data augment strategy and so on.
 1011

1012 **SuS-X:** The generative model of SuS-X is Stable Diffusion V1-4. For a better performance comparion,
 1013 we reimplement SuS-X method with SDXL-Turbo model for higher quality image generation. The prompt
 1014 strategy and other experimental settings keep the setting in the original paper.

1015 **CaFo:** Since CaFo utilizes the OpenAI model to generate description for CLIP text initialization, and the
 1016 original model has been deprecated, we employed the simple template "a photo of {class}" for text ini-
 1017 tialization across all datasets to ensure fairness. All other experimental settings remain consistent with the
 1018 original paper. We have to point that CaFo is a few-shot learning method, and we only report the 16-shot
 1019 result in Table 2 due to space limitation. Other shot results are given in Section D.5.
 1020

1021 D MORE EXPERIMENTAL ANALYSIS

1022 D.1 WHY IS ADAPTIVE PROMPT LEARNING NECESSARY?

1023 To validate the necessity of adaptive prompt selection, we implement two prompt selection baseline strate-
 1024 gies: (1) randomly selecting the same number of prompts from the prompt pool. (2) Using all prompts of the
 1025 prompt pool. Table 4 shows the performance comparison on the STL-10 dataset. All the experiment settings
 1026 are the same as Appendix C.2.3. We can see that the adaptive prompts selected by DeCap method could
 1027 significantly improve classification model performance compared to random selection strategy. Besides,
 1028 although using all prompts in the prompt pool offers more sufficient diversity than subset selection, it suf-
 1029 fers from various issues mentioned in Section 4.3, which may deteriorates the performance of classification
 1030 models. This explains that the performance of all prompts is only better than the random selection strategy
 1031 but not as good as DeCap method. These results further support that adaptive prompt learning strategy is
 1032 more effective in generating high-quality images for downstream few-shot learning tasks.
 1033

Table 4: Comparison of random selection, all selection strategy and DeCap method.

Random	All	DeCap
94.74	95.19	95.90

Table 5: Ablation study on the selecting prompt numbers per class.

5	10	20	40
95.73	95.82	95.90	95.81

Table 6: Ablation study on the number of GA algorithm iterations.

20it	40it	60it	80it
95.73	95.87	95.91	95.90

D.2 ABLATION STUDY

We conducted ablation experiments on two important parameters of our method: the number of prompts selected per class and the iteration count of the GA algorithm. By Table 5, We find that fewer prompts may lead to low dataset diversity, negatively impacting model performance, while more prompts increase optimization difficulty, making it hard to find the optimal solution. We suggest to set the number of prompts selected per class as 20.

Table 6 shows the performance of different numbers of GA algorithm iterations. We observed that performance of classification model converges around 80 generations. In our all experiments, we suggest to set the number of GA algorithm iterations as 80.

D.3 DIFFERENT METRICS

In this section, we give results of other metrics including precision (Table 7), recall (Table 8) and F1-score (Table 9), which are commonly used in few-shot learning, to further explore the robustness and generalization ability of DeCap. Some brief introduction about these metrics are given as follows:

- **Precision:** Precision measures the accuracy of positive predictions. It is defined as:

$$\text{Precision} = \frac{\text{True Positives (TP)}}{\text{True Positives (TP)} + \text{False Positives (FP)}}$$

Precision answers the question: *Of all the instances predicted as positive, how many are actually positive?*

- **Recall:** Recall, also known as sensitivity or true positive rate, measures the ability of the model to correctly identify positive instances. It is defined as:

$$\text{Recall} = \frac{\text{True Positives (TP)}}{\text{True Positives (TP)} + \text{False Negatives (FN)}}$$

Recall answers the question: *Of all the actual positive instances, how many were correctly predicted?*

- **F1 Score:** The F1-score is the harmonic mean of precision and recall, providing a single metric that balances both. It is defined as:

$$F1 = 2 \cdot \frac{\text{Precision} \cdot \text{Recall}}{\text{Precision} + \text{Recall}}$$

The F1-score is particularly useful when the class distribution is uneven or when precision and recall are equally important.

The results demonstrate that our method performs well on these metrics, indicating that it not only achieves high accuracy but also excels in identifying positive samples and is more cautious when dealing with them. It more comprehensively illustrates the robustness and generalization of our method.

1081
 1082
 1083
 1084
 1085
 1086
 1087
 1088
 1089
 1090
 1091
 1092
 1093
 1094
 1095
 1096
 1097
 1098
 1099
 1100
 1101
 1102
 1103
 1104
 1105
 1106
 1107
 1108
 1109
 1110
 1111
 1112
 1113
 1114
 1115
 1116
 1117
 1118
 1119
 1120
 1121
 1122
 1123
 1124
 1125
 1126
 1127

Table 7: **Precision** results of different methods among all datasets.

	vanilla	multi	LE	CiP	DeCap
STL10	95.35	94.90	94.17	95.16	95.63
CIFAR10	76.61	76.55	77.32	77.23	77.40
Im-10	97.27	97.30	97.27	97.30	97.34
Pets	82.58	84.76	84.17	84.52	85.70
Caltech-101	84.42	84.57	85.27	85.39	85.43
Im-100	69.82	71.27	69.28	73.03	71.90
EuroSAT	43.01	38.45	50.50	47.32	49.36
Aircraft	18.38	18.85	20.85	18.67	20.85
Country211	17.20	17.26	18.10	17.12	17.77

Table 8: **Recall** results of different methods among all datasets.

	vanilla	multi	LE	CiP	DeCap
STL10	95.31	94.78	94.04	94.72	95.57
CIFAR10	72.39	69.63	68.24	68.63	76.99
Imagenette	97.25	97.28	97.25	97.28	97.33
Pets	81.69	82.05	82.13	83.12	84.52
Caltech-101	85.21	86.02	85.37	86.07	86.54
Imagenet100	68.32	69.98	67.00	69.56	70.94
EuroSAT	31.07	29.62	28.31	40.62	42.22
Aircraft	17.03	17.84	17.72	17.98	19.71
Country211	13.72	13.90	14.14	14.98	15.44

Table 9: **F1-score** results of different methods among all datasets.

	vanilla	multi	LE	CiP	DeCap
STL10	95.29	94.71	93.99	94.74	95.58
CIFAR10	71.89	69.04	67.30	69.19	76.89
Imagenette	97.23	97.26	97.23	97.26	97.31
Pets	81.28	81.96	82.09	83.23	84.67
Caltech-101	82.04	82.87	82.12	83.45	83.73
Imagenet100	67.06	68.99	65.52	69.42	70.25
EuroSAT	26.36	24.43	24.38	36.36	39.34
Aircraft	15.10	15.98	16.00	15.95	17.81
Country211	13.18	13.35	13.62	14.36	14.93

D.4 ADVERSARIAL ROBUSTNESS

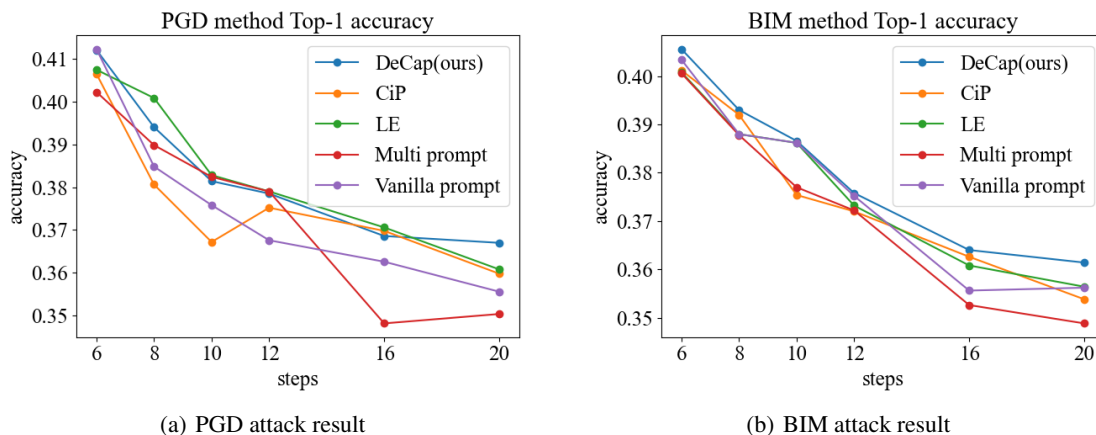


Figure 4: **Adversarial robustness of classification models trained with generated images using different prompts designing methods.** We report the results on the ImageNet100 validation set under two adversarial attack methods. The horizontal axis represents the number of steps taken in the attack, and the vertical axis represents the accuracy of the trained classification model on the validation set after the attack.

Adversarial learning aims to evaluate model robustness by adding small perturbations to the input data, causing the model to make false predictions but making little difference to human observers. We use two common attack methods: BIM (Basic Iterative Method) attack [35] and PGD (Projected Gradient Descent) attack [42]. The BIM employs an iterative gradient ascent approach, where at each step, BIM perturbs the image along the gradient direction predicted by the model. It can be written as $x_{i+1} = x_i + \epsilon \nabla_{x_i} J_{\theta}(x_i, y)$, where x_0 denotes the original image, y denotes its label, and $\nabla_{x_i} J$ means the gradient of loss function w.r.t. x_i . PGD further projects the adversarial examples into an ϵ -ball around the original image.

We use classification model weights obtained from Section 4.1 and implement adversarial attack on ImageNet100 validation dataset. We use torchattacks [32] library to conduct this experiment. We select attack step size ϵ as $1/255$ for these two methods, and Fig.4 reports the attack result on different attack steps. We found that model-generated prompts, due to their rich content details, have a slight advantage in adversarial robustness compared to hand-crafted prompts. Moreover, since DeCap integrates the strengths of hand-crafted and model-generated prompts methods, it consistently performs well in terms of resilience against adversarial attacks.

D.5 MORE EXPERIMENTAL RESULTS OF CaFo AND CaFo + DECAP METHODS

Fig.5 show more experimental results on different shots of each class for CaFo and CaFo + DeCap Methods. The experimental results are aligned with conclusions in Section 4.2.

D.6 ARE PROMPTS WITH DOMAIN INFORMATION ENOUGH FOR CLASSIFICATION?

To illustrate this point, we conducted experiments on the Sketch subclass of the PACS dataset [39]. In this dataset, all images follow the same style. As shown in Fig.6, the hand-crafted prompts could generate sketch-style guitar images, while the image distribution deviates the distribution of real images. This could explain the degraded performance of hand-crafted prompts methods. This is aligned with existing substantial theory

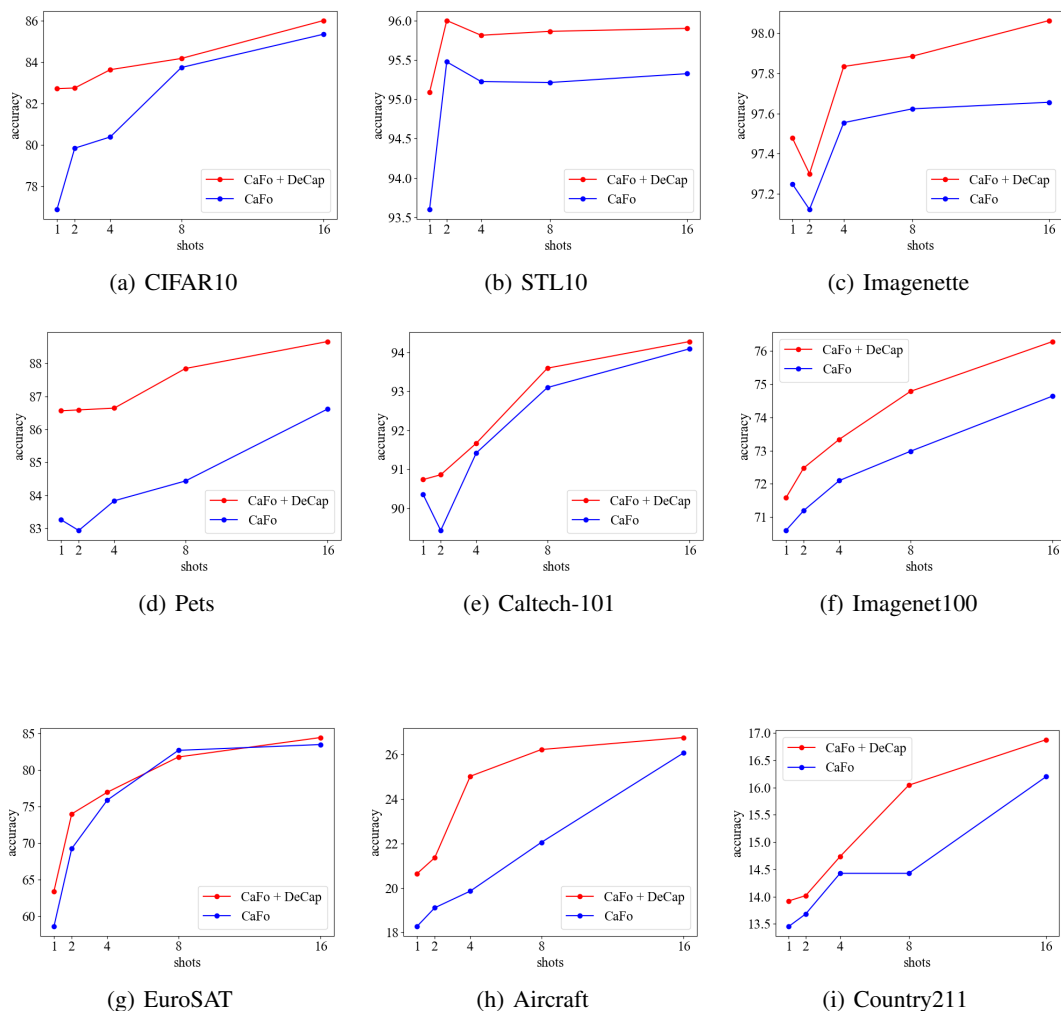


Figure 5: Classification accuracies on different shots of each class for CaFo and CaFo + DeCap Methods

[15; 83; 104], which suggests that samples perfectly matching the real data distribution are most useful for classification. As a comparison, the synthetic images by DeCap method are surprisingly composed of only a portion of sketch-type prompts, supplemented by a significant amount of other types of prompts. The discrepancy between synthetic images and real images is significantly large, however, the performance of classification model training with synthetic data using DeCap method could approach the performance with real data. This result cannot be well explained by existing theories. We hope that a rational theoretical insight could characterize such phenomenon in the future study.

1222
 1223
 1224
 1225
 1226
 1227
 1228
 1229
 1230
 1231
 1232
 1233
 1234
 1235
 1236
 1237
 1238
 1239
 1240
 1241
 1242
 1243
 1244
 1245
 1246
 1247
 1248
 1249
 1250
 1251
 1252
 1253
 1254
 1255
 1256
 1257
 1258
 1259
 1260
 1261
 1262
 1263
 1264
 1265
 1266
 1267
 1268



Figure 6: (Left) Examples of real images, synthetic images by hand-crafted prompts and DeCap methods on PACS Sketch dataset. (Right) Performance comparison between hand-crafted prompts and DeCap methods.

E VISUALIZATION OF SYNTHETIC IMAGES AND LEARNED PROMPTS

E.1 VISUALIZATION OF SYNTHETIC IMAGES

Fig.7 and Fig.8 shows some examples of synthetic images on Pets and Imagenet100 datasets by DeCap method.



Figure 7: Examples of generated images on Pets dataset by DeCap method.

1269
1270
1271
1272
1273
1274
1275
1276
1277
1278
1279
1280
1281
1282
1283
1284
1285
1286
1287
1288
1289

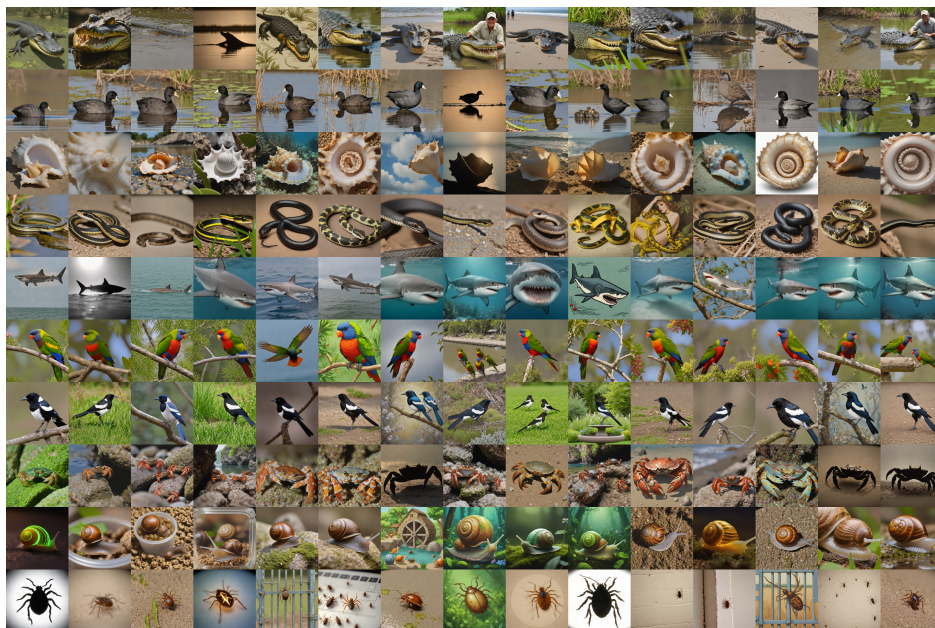
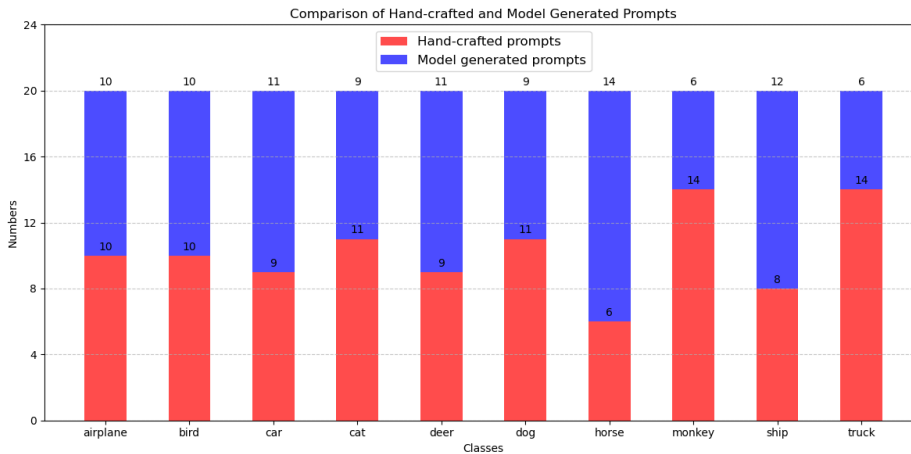


Figure 8: Examples of generated images on Imagenet100 dataset by DeCap method.

1290
1291
1292
1293
1294
1295

E.2 VISUALIZATION OF LEARNED PROMPTS

1296
1297
1298
1299
1300
1301
1302
1303
1304
1305
1306
1307
1308
1309



1310
1311
1312
1313
1314
1315

Figure 9: Illustrations of the number of hand-crafted prompts vs the number of model-generated prompts mined by DeCap method on STL-10 dataset.

We will demonstrate that DeCap method can adaptively learn proper and dataset-specific prompts that are suitable for concerned tasks from the following three aspects.

1316
1317
1318
1319
1320
1321
1322
1323
1324
1325
1326
1327
1328
1329
1330
1331
1332
1333
1334
1335
1336
1337
1338
1339
1340
1341
1342
1343
1344
1345
1346
1347
1348
1349
1350
1351
1352
1353
1354
1355
1356
1357
1358
1359
1360
1361
1362

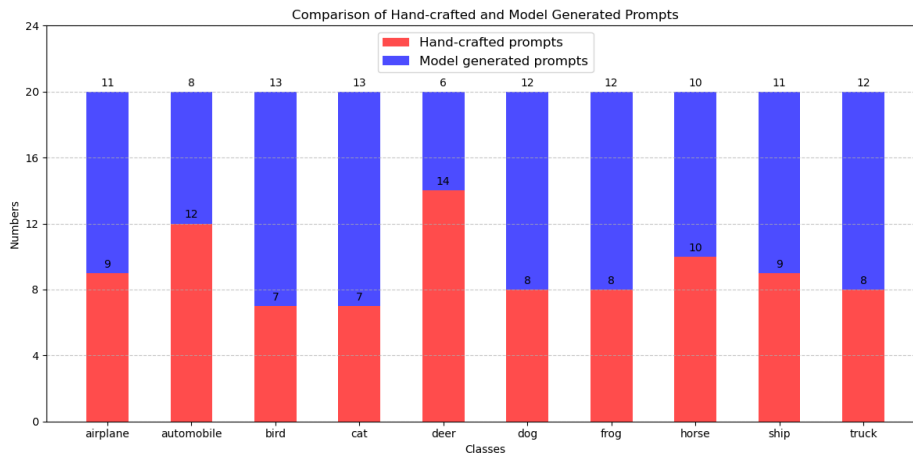


Figure 10: Illustrations of the number of hand-crafted prompts vs the number of model-generated prompts mined by DeCap method on CIFAR10 dataset.

Firstly, the ratios of the number of model-generated and hand-crafted prompts for each class are varying, as shown in Fig. 9 and 10. This reflects that our method could adaptively adjust the proportions that reconcile class/domain information and rich content information for different classes.

Secondly, though the hand-crafted prompts follow the same templates, we can see that different classes may learn relatively different prompts in Fig.11. This further reveals our method could adaptively learn classification-aware prompts for each class, so as to achieve better performance on downstream tasks. **Moreover, we additionally give some examples about the consistently selected model-generated prompts during the optimization process to further highlight the significance of integrating fine-grained prompt descriptions. As we can see in Table 11, the consistently selected prompts show high diversity and fine-grained information, including: movement, posture, background, color, quantity, other objects, and so on. This pictures significantly help to provide classification-benefit features.**

Lastly, Table 10 shows that though STL-10 and CIFAR-10 datasets have some same categories, the learned prompts by our method could be almostly different. This demonstrated that our DeCap method could learning proper prompts suitable to concerned few-shot datasets. For instance, we can see that learned prompts for the STL-10 dataset are realistic, while learned prompts for CIFAR-10 dataset are of low-resolution imagery. Notice that these prompts are well aligned with prior knowledge of these datasets.

Moreover, we additionally display the complete set of prompt pool of the “airplane” class in STL-10 dataset in Table 12, to offer a more intuitive understanding for the characteristic of our method stated above. **And we further give visualizations that demonstrate the prompt selection process over the course of optimization, including image examples and the evolution of prompts, please see Fig.12.**

Table 10: Illustration of mined prompts for “deer” class on different datasets. DeCap method selects completely different prompts for the same class across different datasets, demonstrating its ability to adaptively learn the prompts suited to each specific dataset.

A deer is grazing the woods.
deer are grazing under a tree

1363		a photo of the clean deer.
1364		A silhouette of deer.
1365		a deer and young man roam around during a december game
1366		a photo of a deer.
1367		a deer in a video game.
1368		a toy deer
1369		a deer on a pond
1370		the cartoon deer.
1371		the hornets and deer are on a ridge
1372		a deer.
1373		deer resting with the grazing padou atop old farmhouse
1374		An ink painting of a deer
1375		deer on a green pond.
1376		the toy deer.
1377		a brown bear eats the deer
1378		A glossy deer.
1379		a photo of a large deer.
1380		a group of deer on prairie are seen grazing in their natural habitat
1381		a photo of deer, a wild deer in the wild
1382		a deer on a farm
1383		A soft-focus deer.
1384		art of a deer.
1385		deer and their prey on the northern slopes
1386		a photo of deer, a deer standing in the snow with a sky background
1387		a pixelated photo of the deer.
1388		several deer grazing in the desert
1389		fox and a deer on the grounds of a city
1390	CIFAR10	a rendering of a deer.
1391		a photo of deer, a group of deers standing in a field
1392		A silhouette of deer.
1393		a photo of deer, a deer is standing in the grass
1394		a deer is grazing an ancient inscription.
1395		a photo of deer, a herd of deer in the desert
1396		deer and the munro.
1397		A pair of deer on a trail.
1398		a hunt deer on a desert land
1399		deer and the munro.
1400		a pixelated photo of the deer.
1401		
1402		
1403		
1404		
1405		
1406		
1407		
1408		
1409		

1410
1411
1412
1413
1414
1415
1416
1417
1418
1419
1420
1421
1422
1423
1424
1425
1426
1427
1428
1429
1430
1431
1432
1433
1434
1435
1436
1437
1438
1439
1440
1441
1442
1443
1444
1445
1446
1447
1448
1449
1450
1451
1452
1453
1454
1455
1456

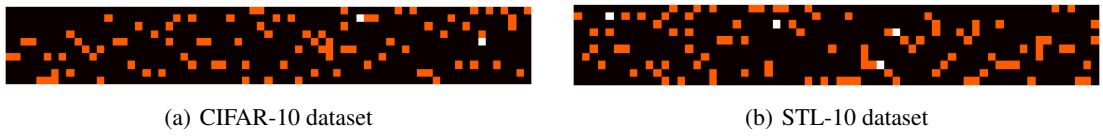


Figure 11: Illustration of mined hand-crafted prompts for each class by DeCap method across two datasets. Each column represents the same template, and each row indicates which prompts were selected for class of this row. Black indicates prompt is not selected, orange indicates the prompt is selected once, and white indicates the prompt is selected more than once. For clarity, we removed prompts that were not selected by any class of the dataset. It could be observed that although the prompt templates are the same, the domain information required by each class is distinctly different, demonstrating DeCap’s ability to adaptively learn suitable prompts for the classification of each class.

Table 11: **Examples of model-generated prompts which are consistently selected during optimization process.**





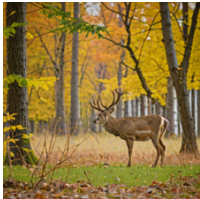
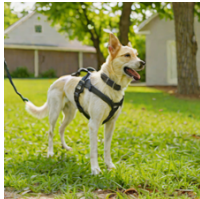



<p>a bird sitting on a branch.</p> 	<p>cars that have to make an effort to turn off.</p> 	<p>A black cat is in a room where the window is down.</p> 
<p>A truck with lots of people on it.</p> 	<p>A deer is grazing the woods.</p> 	<p>A dog is standing in its yard with a harness on it.</p> 
<p>A white horse in the open barn.</p> 	<p>dogs inside a home on a summer.</p> 	<p>a semi truck driving down a rural road.</p> 

Table 12: The prompt pool of “airplane” class in STL-10 dataset. Mined prompts by DeCap method are highlighted in **bold**.

Model-generated prompts

1457

1458

1459

1460

1461

1462

1463

1464

1465

1466

1467

1468

1469

1470

1471

1472

1473

1474

1475

1476

1477

1478

1479

1480

1481

1482

1483

1484

1485

1486

1487

1488

1489

1490

1491

1492

1493

1494

1495

1496

1497

1498

1499

1500

1501

1502

1503

a photo of airplane , a small plane is parked on the runway	a photo of airplane , a large passenger jet flying through a blue sky	a photo of airplane , a small plane is on the runway	a photo of airplane , a yellow airplane flying through a blue sky
a photo of airplane , a large passenger jet flying through the sky	a photo of airplane , a small plane flying in the sky	a photo of airplane , a small plane is floating in the water	a photo of airplane , a large passenger jet sitting on a runway
a photo of airplane , a small plane flying in the sky	a photo of airplane , a small blue airplane is taking off from the runway	a photo of airplane , a plane is parked on the tarmac	a photo of airplane , two small planes are sitting on the water
a photo of airplane , a plane flying in the sky	a photo of airplane , a small plane flying over a mountain range	a photo of airplane , a plane is on the runway	a photo of airplane , a small plane flying through the air
a photo of airplane , a large white plane	a photo of airplane , two planes flying in the sky	a photo of airplane , a plane flying in the sky	a photo of airplane , a small plane flying over a city
a photo of airplane , a plane flying in the sky	a photo of airplane , a small plane flying through the air	a photo of airplane , a plane flying in the sky	a photo of airplane , a plane is parked on the tarmac
a photo of airplane , a plane flying in the sky	a photo of airplane , a plane flying in the sky	a photo of airplane , a small plane is parked on the water	a photo of airplane , a plane flying in the sky
a photo of airplane , a small plane sitting on a snowy field	a photo of airplane , a small plane flying in the sky	An airplane that has been seen flying over another airplane.	A plane is in a parking lot.
airplane that you bought a few years ago	A small airplane is flying over a highway at a time.	An airplane that is parked in an airport	The plane has an engine, a seat, a console, a charger, and
An aircraft is in the flight over a lake.	The airplanes are all parked inside the parking lot.	A plane is in the air.	plane of a small aircraft.
A red and white airplane with a green and green color scheme.	An airplane parked on the runway near a pier.	An airplane that has just broken ground behind it.	A plane parked next to one of the airplanes above it's engine.
Airplanes in space that are not as big as usual.	An airplane parked along a highway.	A small airplane that's flying at low speeds under a cloudy sky.	airplanes need people to work hard at the zoo
An airplane parked next to a bridge.	Some airplanes flying over people.	The airplane is in a green sky with blue skies.	The airplane with the lights is about to be docked.
An airplane with three engines and a propeller.	an airplane with a window	An airplane parked on top of a hill next to it	airplane on the tracks.
An airplane on an airplane track	A plane with tires on it flying away from it.	An airplane is parked on a runway at a airport.	These airplanes are in a wing.
a commercial airplane traveling in july.	airplane in flight... a photo and video	Two air planes all flying in a row.	A modern airplane is arriving in the air.
An airplane in the middle of nowhere with its doors lowered.	airplane is parked in a parking lot	An airplane that is coming in to land.	passengers in an airplane in the rain

1504	1505	1506	1507	1508	airplanes flying at a rate of 2 to 3 mph on a Sunday	An airplane on a runway next to a small green field.	an airplane on an airport runway	a classic red blue airplane is shown in the cockpit with bright colors as well.
1509	1510	1511	1512	1513	planes in a dry pit	airplane and other objects in the air	an airplane makes an outgoing landing on the ground	An old airplane is coming down the track.
1514	1515	1516	1517	1518	A man attempting to board a commercial airplane.	Small airplanes with wing lights attached to them.	A small airplane with the tail mounted up.	An airplane in a flight path with some passengers nearby.
1519	1520	1521	1522	1523	airplane on an old building	An aircraft goes up through a window dripping with smoke and debris.	airplanes that have been converted to jet engines	airplanes cruising in the bay.
1524	1525	1526	1527	1528	A boy is running with an airplane that is on the runway.	A blue airplane has its wings shut.	An airplane is about to land in a parking lot and be delivered.	two airplanes parked at the airport
1529	1530	1531	1532	1533	A white airplane on the runway with blue ice.	jet airplane is ready for a test	An airplane is sitting on a ground with all three engines on the ground.	There's one airplane in the cockpit which is parked by another airplane.
1534	1535	1536	1537	1538	An airplane is in the air.	A family is on a small airplane at a hotel.	aircraft carrier and an airplane together with some gulls.	airplane inside of the airplane
1539	1540	1541	1542	1543	The airplane is looking down.	An airplane is shown flying on a runway.	small bodied airplane on a plane	An airplane parked next to fireworks on the sky.
1544	1545	1546	1547	1548	An airplane that appears to be on the runway.	An airplane that is very close to the ground in an airport.	Various aircraft and airplanes are getting ready for flight.	an airplane is seen arriving on a runway
1549	1550				Two aircrafts in a white airplane at a station.	The airplane landed.	an airplane that is making a flying flight	airplane on the runway at the airport
					this airplane was able to take off with just a small amount of effort to get the	An airplane that is in a flying position.	An airplane making its way between jets.	airplane sitting in air
					a large old plane sits off the fuel tank	aircraft carrier and its crew arriving in an airplane	airplane on the runway	A family of airplanes are in a building.
					plane flies around city	an airplane about to land in a desert	An electric airplane in the sky.	an airplane that is making it's way around the tarmac
					airplanes on the runway	the crew of airplane on board	The airplane is in the air.	jet airplane wing during maintenance
					A blue and white airplane with white wing panels.	A commercial airplane flying under the radar.	The airplane has been damaged by the winds.	An airplane flying near a tarmac.

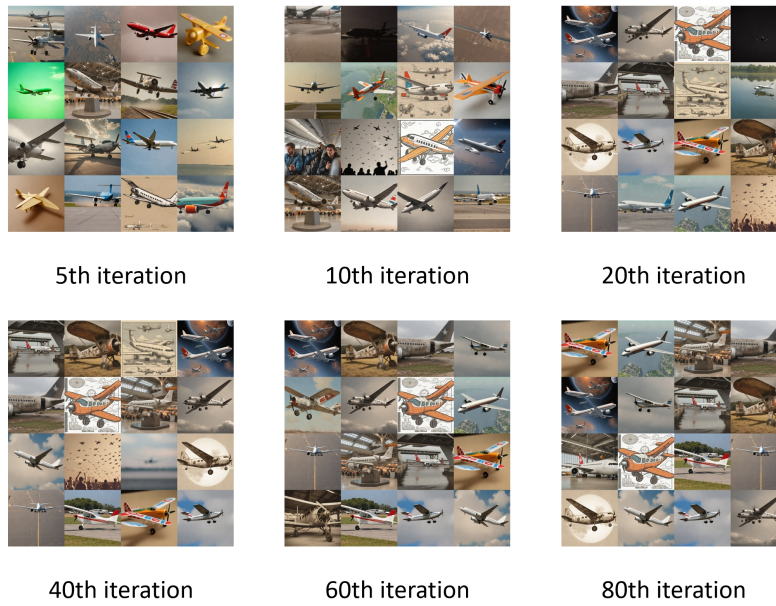
Hand-crafted prompts

1551				
1552	a good photo of the airplane.	a photo of many airplane.	a sculpture of a airplane.	a photo of the hard to see airplane.
1553				
1554	a low resolution photo of the airplane.	a rendering of a airplane.	graffiti of a airplane.	a bad photo of the airplane.
1555				
1556	a cropped photo of the airplane.	a tattoo of a airplane.	the embroidered airplane.	a photo of a hard to see airplane.
1557				
1558	a bright photo of a airplane.	a photo of a clean airplane.	a photo of a dirty airplane.	a dark photo of the airplane.
1559				
1560	a drawing of a airplane.	a photo of my airplane.	the plastic airplane.	a photo of the cool airplane.
1561				
1562	a close-up photo of a airplane.	a black and white photo of the airplane.	a painting of the airplane.	a painting of a airplane.
1563				
1564	a pixelated photo of the airplane.	a sculpture of the airplane.	a bright photo of the airplane.	a cropped photo of a airplane.
1565				
1566	a plastic airplane.	a photo of the dirty airplane.	a jpeg corrupted photo of a airplane.	a blurry photo of the airplane.
1567				
1568	a photo of the airplane.	a bad photo of a airplane.	a rendering of the airplane.	a airplane in a video game.
1569				
1570	a photo of one airplane.	a doodle of a airplane.	a close-up photo of the airplane.	a photo of a airplane.
1571				
1572	the origami airplane.	the airplane in a video game.	a sketch of a airplane.	a doodle of the airplane.
1573				
1574	a airplane.	a origami airplane.	a low resolution photo of a airplane.	the toy airplane.
1575				
1576	a rendition of the airplane.	a photo of the clean airplane.	a photo of a large airplane.	a rendition of a airplane.
1577				
1578	a photo of a nice airplane.	a photo of a weird airplane.	a blurry photo of a airplane.	a cartoon airplane.
1579				
1580	art of a airplane.	a sketch of the airplane.	a embroidered airplane.	a pixelated photo of a airplane.
1581				
1582	a jpeg corrupted photo of the airplane.	a good photo of a airplane.	a photo of the nice airplane.	a photo of the small airplane.
1583				
1584	a photo of the weird airplane.	the cartoon airplane.	art of the airplane.	a drawing of the airplane.
1585				
1586	a photo of the large airplane.	a black and white photo of a airplane.	a dark photo of a airplane.	graffiti of the airplane.
1587				
1588	a toy airplane.	a photo of a cool airplane.	a photo of a small airplane.	a tattoo of the airplane.
1589				
1590	a digital style airplane	a colorful airplane	a modern style airplane	an abstract photo of airplane
1591				
1592	a cartoon style airplane	a virtual style airplane	An ink painting of a airplane	a toy airplane
1593	A model airplane.	a red airplane	a blue airplane	a yellow airplane
1594	a black airplane	a white airplane	An old airplane.	A futuristic airplane.
1595				
1596	A minimalist airplane.	A detailed illustration of airplane.	A close-up of airplane.	A shadowy figure of airplane.
1597				
1598	A silhouette of airplane.	A bright and vibrant airplane.	An abstract concept of airplane.	A vintage style airplane.

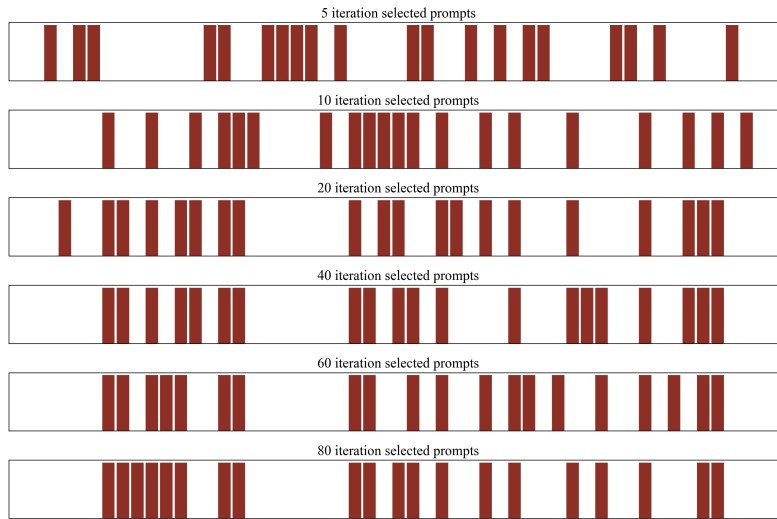
1598
1599
1600
1601
1602
1603
1604
1605
1606
1607
1608
1609
1610
1611
1612
1613
1614
1615
1616
1617
1618
1619
1620
1621
1622
1623
1624
1625
1626
1627
1628
1629
1630
1631
1632
1633
1634
1635
1636
1637
1638
1639
1640
1641
1642
1643
1644

A neon-lit airplane.	A monochrome airplane.	A watercolor painting of airplane.	A sketch of airplane.
A digital art of airplane.	A handcrafted airplane.	An aerial view of airplane.	A side profile of airplane.
A textured airplane.	A glossy airplane.	A matte airplane.	A glowing airplane.
A rustic airplane.	A weathered airplane.	A sparkling airplane.	A serene airplane.
A chaotic airplane.	A whimsical airplane.	A dynamic airplane.	A frozen moment of airplane.
A soft-focus airplane.	A high-contrast airplane.	A sepia-toned airplane.	A saturated airplane.
An isolated airplane.	A mirrored airplane.	A panoramic view of airplane.	An enchanted airplane.

1645
1646
1647
1648
1649
1650
1651
1652
1653
1654
1655
1656
1657
1658
1659
1660
1661
1662
1663
1664
1665
1666
1667
1668
1669
1670
1671
1672
1673
1674
1675
1676
1677
1678
1679
1680
1681
1682
1683
1684
1685
1686
1687
1688
1689
1690
1691



(a) Image examples during different optimization iterations.



(b) The evolution of prompts during different optimization iterations.

Figure 12: Image examples and the evolution of prompts during different optimization iterations. For clarify, Fig.(b) shows only the selected prompts and omits the rest.

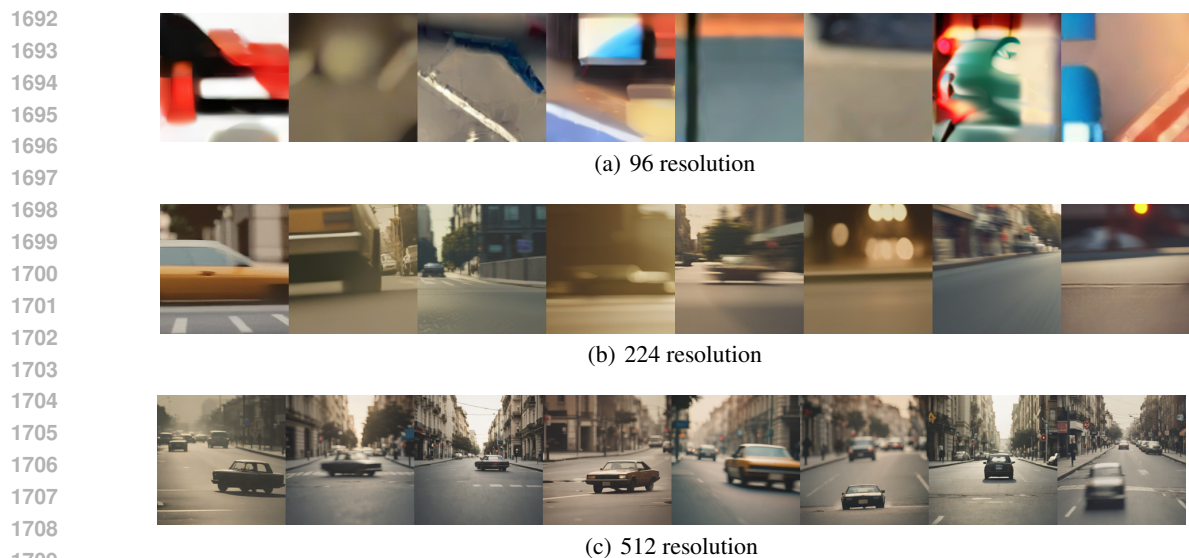


Figure 13: prompt: “a photo of a car in the street”

1710
1711
1712
1713 **F REBUTTAL DISPLAYS**

1714
1715 This section is just for additional rebuttal visualization.

1716
1717 **F.1 DIFFERENT RESOLUTIONS**

1718
1719 We give some examples about generating images using different resolution in Fig.13. We can see that
1720 generative large models are only good at the resolution of its training set, i.e. 512 resolution.
1721

1722
1723
1724
1725
1726
1727
1728
1729
1730
1731
1732
1733
1734
1735
1736
1737
1738